LAPPEENRANTA UNIVERSITY OF TECHNOLOGY
Department of Chemical Engineering
Master's Thesis
2016

Shoaib Khan

Synthesis of high capacity adsorbents from low-cost materials, with atomic layer deposition, for mine water treatment

Examiner: Prof. Mika Sillanpaa
Supervisor: M. Sc. Evgenia Iakovleva

ABSTRACT

Lappeenranta University of Technology

School of Engineering Science

Degree Program of Mechanical Engineering

Shoaib Khan

Synthesis of high capacity adsorbents from low-cost materials, with atomic layer deposition, for mine water treatment

Master's Thesis

2016

91 pages, 40 figures, 13 tables

Examiner: Prof. Mika Sillanpää

Supervisor: M. Sc. Evgenia Iakovleva

Keywords: acid mine drainage; adsorption; atomic layer deposition

Abstract

Mining waste water with all its harmful effects is an ongoing problem for the ecosystem, hence methods are proposed to bring this issue to an end. Among these methods are trying out a number of low cost adsorbents, potentially industrial wastes, which can be altered somehow to get better adsorption properties. The aim of this thesis work is to improve the adsorbent capacities of certain low cost adsorbents, by some modification done by atomic layer deposition. ZnO, TiO_2 and Al_2O_3 films were deposited on granules and fine powders of these adsorbents and tested on synthetic and real AMD water for the removal of Cu^{2+}, Fe^{3+}, Zn^{2+}, Ni^{2+}, SO_4^{2-} and CN^- ions. Modified industrial solid waste (iron sand) was used to remove metallic ions from real mine water and the percentage removed was 50%, 75%, 80%, 99% and 90 for SO_4^{2-}, Ni^{2+}, Zn^{2+}, Fe^{3+} and Cu^{2+} respectively. Modified sulfate tailings were used to remove cyanide from synthetic mine water, removal efficiency of around 97% was achieved, selectively removing cyanide ions from synthetic mine water.

TABLE OF CONTENTS

LIST OF FIGURES

LIST OF TABLES

ABBREVIATIONS

AMD	Acid mine drainage
ALD	Atomic layer deposition
GDP	Gross domestic product
USGS	United States geological survey
NAG	Net acid generation
NAPP	Net acid production potential
MCL	Maximum Contaminant Levels
AFM	Atomic Force Microscopy
SEM	Scanning Electron Microscope
FTIR	Fourier Transform Infrared spectroscopy
BET	Brunauer–Emmett–Teller analysis
XRD	X-ray diffraction
HPLC	High precision liquid chromatograph

1. INTRODUCTION

1.1. Background

The mining industry continues to grow further with new extraction methods being employed to meet the demands of hungry industries relying for processed materials. Countries rich in mineral resources contribute a lot and have their influence in development of many relying industries such as construction, electronics and nearly everything touch our lives. However, there is one other side to this excavation, the mine waste water, the consequences of which have recently been acknowledged and much research has been spent over years for remedial measures.

Recently a lot of emphasis is paid over the potential use of solid wastes from different industries for the removal of contaminant ions from mine water. Adsorption phenomenon has developed as one of the main removal methods for a wide range of contaminants, with the global slogan of BANTEEC (Best Available Technology Not Entailing Excessive Cost), research based on new findings for cheap and most effective adsorbents continues (McKay, 1996). Industrial wastes containing iron compounds, possibly oxides, have been found quite consistent with removal of several contaminants.

Atomic layer deposition has received attention recently in electronics industry, for its unique ability to develop monolayers onto the substrates with good surface uniformity. This process can thus be utilized to develop very fine layers of desired oxides onto a number of materials for potential use as adsorbents, being the objective of this study, where very fine nano-layers of Al_2O_3 and TiO_2 are deposited onto industrial wastes to treat min water.

1.2. Objectives of the Study and Research questions

The main aim of this study was to synthesize advanced materials by atomic layer deposition in order to treat mine water. Industrial byproducts already established as good adsorbents in recent studies, such as iron sand and sulfate tailings are put into use to minimize the environmental impact (Iakovleva et al., 2015). The process is carried out creating various TiO_2 and Al_2O_3 thin films onto these materials and their physical and chemical characterization with respect to the original materials. Finally, the modified materials are tested for synthetic and real mine water. The research is divided into two parts, first one being synthesis and characterization of modified iron sand for removal of Ni^{+2}, Cu^{+2}, Zn^{+2}, Fe^{+3} and SO_4^{-2} from real and synthetic acid mine drainage (AMD). Secondly preparation and characterization of modified sulfate tailings for removal of cyanides from synthetic mine water. Following characterization methods were used, results generated based on experiments scanning electron microscopy (SEM), Fourier Transform Infrared Spectroscopy (FTIR), Brunauer–Emmett–Teller Analysis (BET), Atomic Force Microscopy (AFM) and X-Ray Diffraction (XRD).

Before starting the research following research questions may arise which will be answered by this study.

- *Why do we need to carry out mine water treatment?*
- *What other industrial byproducts have already been employed for treating waters?*
- *Why select adsorption as the mine water treatment phenomenon?*

The purpose of this study is to extend the understanding of possibility of usage of industrial byproducts for treating mine water related issues.

1.3. Research Structure

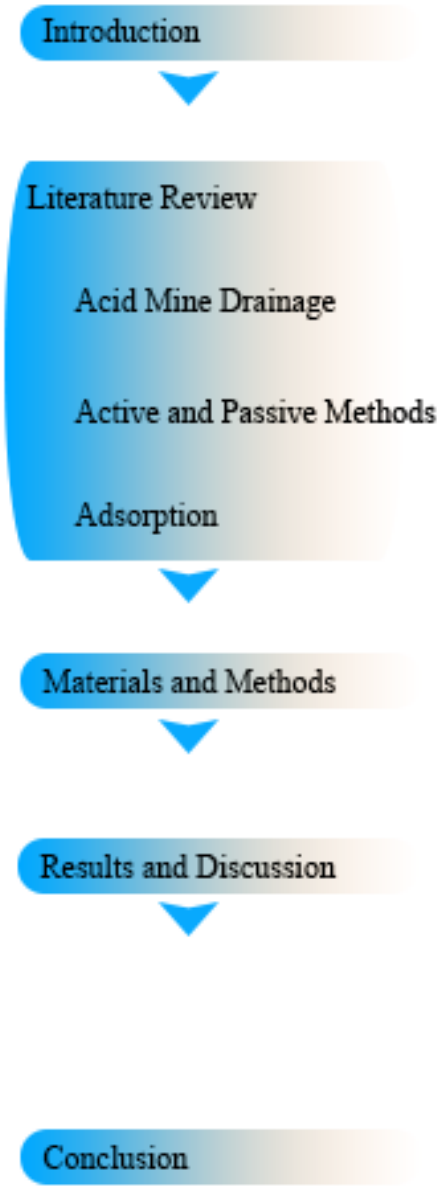

Research background and motives.

Role of mining industry in AMD generation, basic concepts regarding generation of acid mine drainage. Current methods for the treatment and comparison with adsorption process. Basics of adsorption process and isotherms. Some of the low-cost adsorbents currently used, a short briefing of industrial byproducts being used as adsorbents.

Materials utilized, their preparation, equipment used. Synthesis of adsorbents by atomic layer deposition.

Characterization methods used, results generated based on experiments SEM, FTIR, BET, AFM, XRD. Adsorption experiments on real and synthetic mine water, comparison of real and modified adsorbents.

Final remarks on base of experimental data, whether the process is applicable and some future to this kind of research.

2. LITERATURE REVIEW

2.1. Mining Industry and Waste Water

The mining industry of any country has as a great impact on overall gross domestic product (GDP), for example for Austria alone it went from 7.9% to 9% from 2010 to 2011, however the European share in mining falls behind the US and it doesn't contribute to that extend in GDP (Minerals Yearbook - Area Reports: International Review, 2013).

The European parliament and the council of the European union has this predefined set of regulations for mining industries operating within Europe, which includes action to be taken by member States against the abandonment and mismanagement of extractive wastes at mines, which also is accountable to maintain a check on waste management plans to be prepared by the operator including treatment, recovery and proper disposal of all the wastes (European parliament and of the council, 15 March 2006). Finland is one the leading mining country in Europe, in paper industry for instance the production of talc and resources of carbonates used as pigments. Table 1 shows the minerals being produced in Finland, amongst these Zinc, Copper, Chrome and nickel are worth mentioning (Geological survey of Finland, 2016).

According to statistics shown in figure 1 collected in 2014, the wastes generated as a result of mining operations in Europe amounts to be 774 million tonnes which contributes to about 29.8% of the total waste produced. The waste distribution among countries was the highest among having relatively larger mining operations such as Bulgaria, Sweden, Finland and Romania (Ec.europa.eu, 2016). As majority, as much as 99% for some low-grade metal ores, of the material being extracted end up tailings generally during the processing of the ore. The size of tailings depends on the sorting and processing operations it went through. The content however depends on what time of mineral enrichment it was produced.

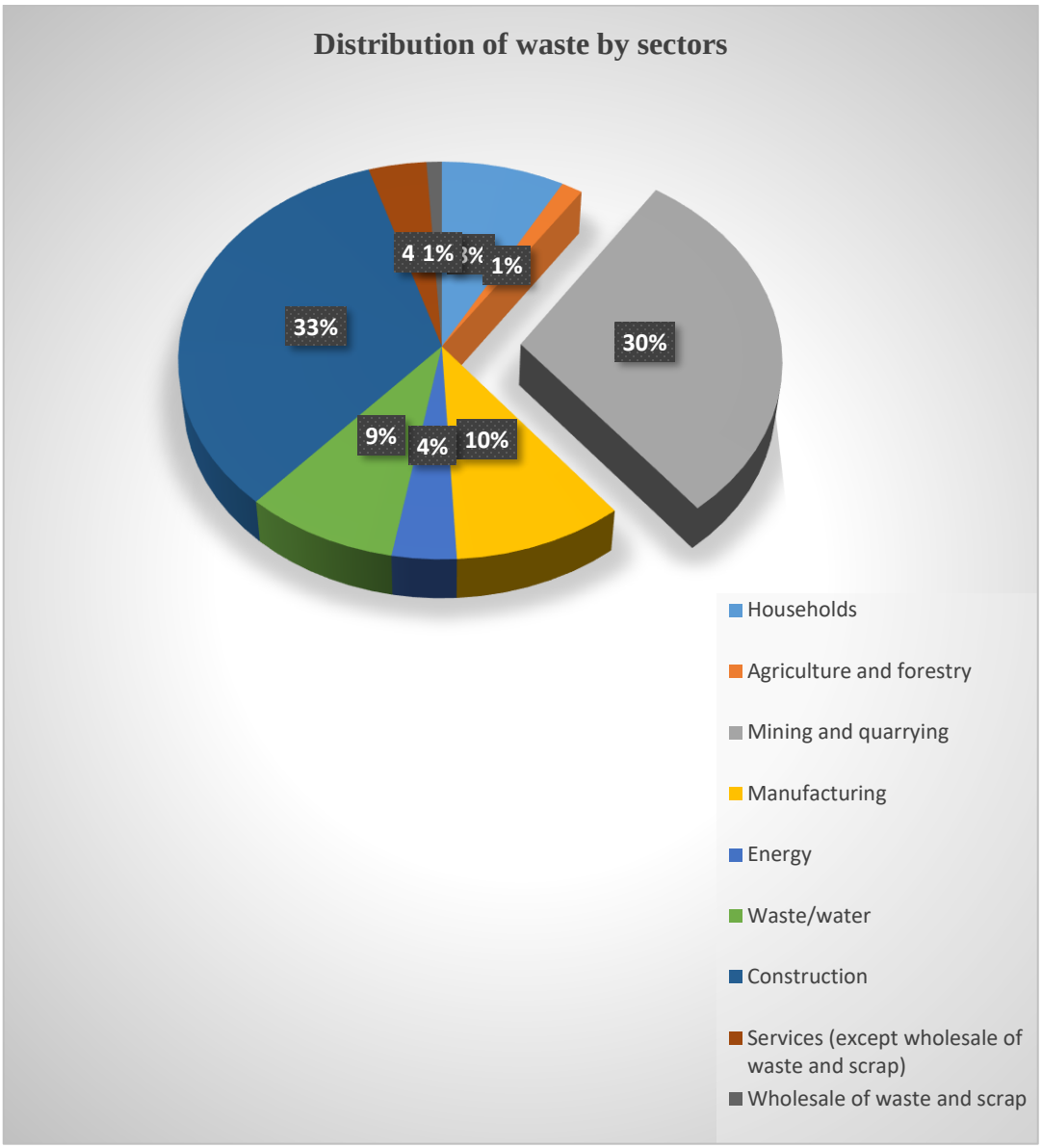

Figure 1. Shares of different sectors contributing waste in European countries (Modified from Ec.europa.eu, 2016).

The waste generated by the industry as a whole, around 57% comes from mining activities. The figure 2 shows the percentage amount of the waste generated by a country based on mining, manufacturing and power generation. For example, for Finland it can be seen more than 50% of waste generated by industries is mining related (Ec.europa.eu, 2016). According to this data most of the waste generated is inert or has no direct impact on environment, 0.4% is hazardous, still if carried through water streams makes it quite a concern.

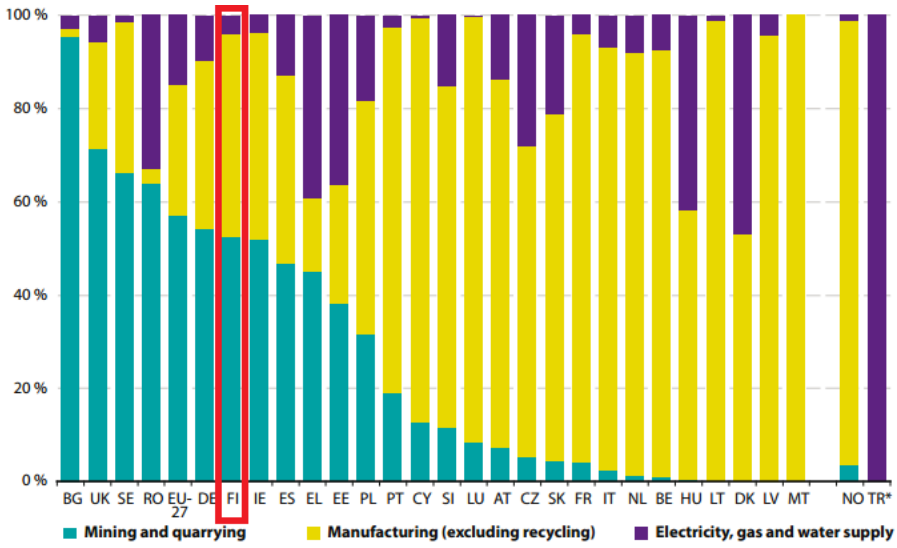

Figure 2. Percentage contribution of different industries in waste production, with Finland highlighted in red (Modified from Ec.europa.eu, 2016).

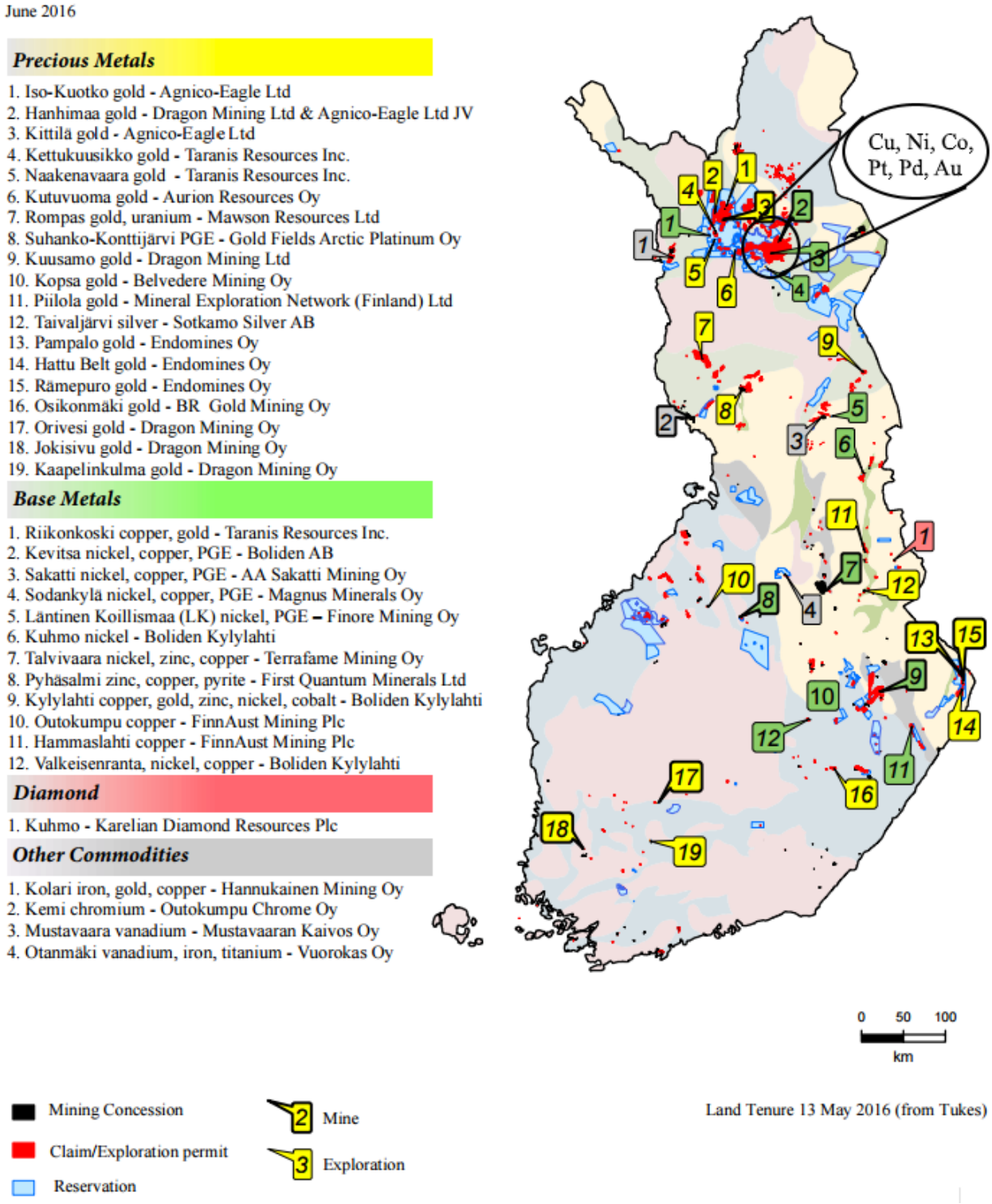

Figure 3. List of ongoing mining projects in Finland (Modified from (Geological survey of Finland, 2016))

The mining operations go all around in Finland generating solid wastes, having harmful impact on the environment. Figure 3 shows the map for the mining operations being carried as observed by geological survey of Finland. Sulfate tailings produced by some mining processes have been utilized in this studies, with modification they have been successfully used to treat synthetic mine water. The mine water has more environmental concerns because of dissolved metallic ions at proportions lot more than safe. Table 1 below shows the timeline for wastes generated, from 1999 to 2012 during mining operations for respective metals in Finland alone.

Table 1. Wastes from metal mine (modified from Reichl, 2014).

Finland — Wastes generated, from 1999 to 2012, during mining operations for respective metals in Finland

Mineral	1999	2000	2001	2002	2003	2004	2005	2006	2007	2008	2009	2010	2011	2012
Copper [t]		10810	11555	14400	14900	15500	15000	13000	13600	13300	14600	14700	14100	30300
Gold [kg]	3159	5220	1495	1600	1550	1360	1296	1307	1639	1336	1500	2000	8461	10814
Nickel [t]		1916	2027	3500	3229	3400	3386	2985	6465	4303	4400	12100	19100	20000
Platinum [kg]				508	461	705	678	711	461	214	265	300	373	709
Silver [kg]	22000	15000	8389	29900	33960	49400	47500	50800	44900	69900	69600	69600	73081	128200
Zinc [t]	19751	17500	20131	34100	39850	37200	40803	35700	38900	27800	30900	55600	64100	52200
Feldspar [t]		38609	35995	40000	58353	57149	52383	43187	48980	45250	45000	45000	26292	43124
Sulphur [t]	415802	414371	303808	288879	665980	674220	559150	595493	645000	707300	710000	644000	791300	830000
Talc [t]	508770	501853	476620	477000	501658	528943	508169	547146	535882	550000	550000	550000	429494	396332

Fresh water deposits are getting scarce, as there is a climate change due to global warming. The deposits we have now are being contaminated by all sorts of wastes among which mine water is most alarming. Water resources are being depleted in some regions due to depletion of rainfall. Therefore, safeguarding of existing resources is of extreme importance. Being chemically and biologically indestructible, the overdose of heavy metallic ions is inevitable unless proper measures are taken. A complete understanding of the behavior of these elements in human body is therefore needed, with their uses in different metabolism processes, their

deficiency and overdose is needed to be taken into account before planning proper water treatment operation.

In European countries for instance this problem is of extreme importance as there are a number of countries exposed to very toxic contaminated waters, for examples, Czech Republic faces contamination with barium, nickel and selenium, Lithuania with iron, Chile, Slovakia and Hungary with arsenic (Ferrante et al., 2013). Despite the scale provided by the World Health Organization (WHO) majority of people across the world drink water having more than 10 parts per billion (ppb) of arsenic, the limit already set by WHO. The standards however are not revised in many less developed countries, which still carry out 50 ppb as frame of reference for actions to purify water (Rgs.org, 2017).

In Pakistan for instance one of the major contributors to the pollution in water is Fe. A survey shows the excess of iron in both surface and subsurface water, nearly 28% and 40% respectively. Apart from iron, cadmium, nickel, lead and mercury were found in some parts of country exceeding the standard allowed limit. But the pollutant with highest concentration is arsenic (As), with nearly most of regions the concentration exceeds the WHO limit of 10 ppb. For example, according to tests carried out by Pakistan Council for Research in Water Resources (PCRWR), in cities like Multan nearly 50% samples were found to be polluted more than allowed limit (Azizullah et al., 2011). Another studies relevant to a coal mine reveals the possible leaching of elements such as silicon, aluminum, sulfur and iron. Trace elements included As, Cd, Co, Cr, Cu, Pb and Zn showing considerable range for generation of AMD (Qureshi, Maurice and Öhlander, 2016).

The corrosive nature of these waters is also a concern, falling in low pH can cause extremely corrosive conditions as a case study suggests in India (Singh, 1986). For instance, the concentrations of dissolved ions in underground water is found to be a lot higher than permissible limits because of higher than normal discharge of effluents which are not monitored properly in these countries (Siddharth et al., 2002).

As mining industry continues to employ new techniques to harvest all sorts of materials used in industrial applications as well as household stuff, which creates demand for more excavation of earth for attaining these materials. The table 2 below shows the trend of production of some

minerals produced over years, their production in year 1999 is compared to year 2006. Both underground and open cast methods are under use of mining industry, however the later one generates comparatively more mining waste. Extraction of metalliferous materials is of quite concern since a very low quantity is derived from the basic ore for example, just as an estimation, on ton of copper extraction may produce around 110-ton waste, as compared to production of sand and clay where nearly all of the material extracted is put to some use somehow (Lottermoser, 2007).

Table 2. World production of minerals 1999 and 2006, with a few metals in interest highlighted (Modified from USGS 2001, 2009).

Mineral or product	Production 1999	Production 2006	Mineral or product	Production 1999	Production 2006
Antimony	0.122 Mt	0.134 Mt	Asbestos	1.93 Mt	2.3 Mt
Arsenic trioxide	38800 t	52700 t	Barite	5.66 Mt	7.96 Mt
Bauxite	127 Mt	178 Mt	Bentonite	9.82 Mt	11.7 Mt
Beryl	6210 t	4480 t	Boron minerals	6.37 Mt	4.26 Mt
Chromite	14 Mt	19.7 Mt	Cement	1610 Mt	2560 Mt
Cobalt	29900 t	67500 t	Feldspar	8.98 Mt	15.4 Mt
Copper	12.6 Mt	15.1 Mt	Fluorite	4.51 Mt	5.33 Mt
Gold	2540 t	2460 t	Fuller's earth	3.52 Mt	3.98 Mt
Iron ore	990 Mt	1800 Mt	Graphite	0.685 Mt	1.029 Mt
Lead	3.02 Mt	3.47 Mt	Gypsum	106 Mt	12.5 Mt
Manganese ore	20.4 Mt	33.4 Mt	Kaolinite	41.6 Mt	37.5 Mt
Mercury	1800 t	1480 t	Lime	141 Mt	271 Mt
Molybdenum	0.123 Mt	0.185 Mt	Magnesite	10.7 Mt	14.1 Mt
Nickel	1.12 Mt	1.58 Mt	Mica	0.304 Mt	0.342 Mt
Niobium–tantalum concentrate	57100 t	67700 t	Peat	27.2 Mt	25.8 Mt
Platinum-group elements	379 t	518 t	Perlite	1.85 Mt	1.81 Mt
Silver	17700 t	20200 t	Phosphate rock	141 Mt	142 Mt
Tin	0.198 Mt	0.304 t	Potash	25.7 Mt	29.1 Mt
Titanium concentrates	4.17 Mt	6.7 Mt	Salt	209 Mt	251 Mt
Tungsten	31000 t	90800 t	Sand and gravel	107 Mt	117 Mt
Vanadium	42200 t	56300 t	Sulfur	57.1 Mt	65.7 Mt
Zinc	8.04 Mt	10 Mt	Vermiculite	0.534 Mt	0.518 Mt

Figure 4 shows the typical types of wastes produced while extraction of the ore, as we dig deep there is a huge amount of waste from topsoil, overburden and then country rocks. The rest comes with mineral processing as tailings, and finally when the metal is seperated through metallurgical processes in form of slags (Lottermoser, 2007).

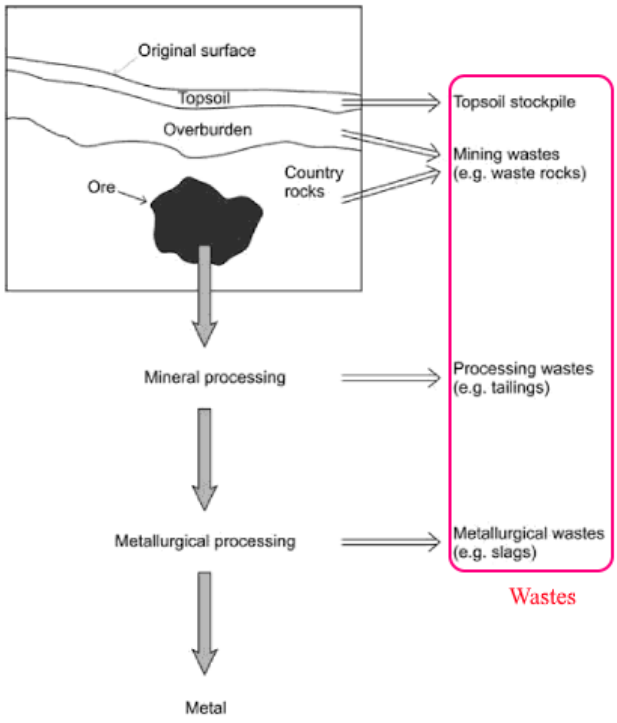

Figure 4. Wastes from metal mine (Modified from Lottermoser, 2007).

Figure 5 shows the waste emissions produced by the two metallurgical processes hydrometallurgical and pyrometallurgical., the later uses heating to separate the metal from the ore but the waste produced as slags, waste waters, leached ore and roasting products (Lottermoser, 2007). Insufficient resources to treat the remaining ore, vast amounts are sent for landfills potentially polluting the ground water (Iakovleva et al., 2015).

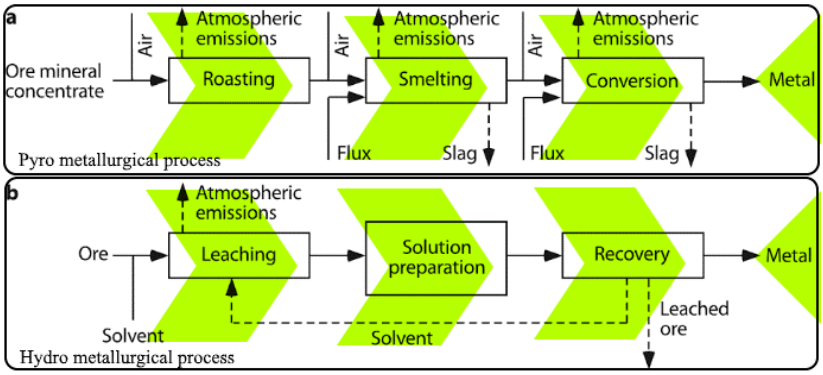

Figure 5. a) Pyro metallurgical and b) hydrometallurgical process (Modified from Lottermoser, 2007).

An assessment of the lands or places affected by mine wastes can thus be made through experimentation. The way it affects the humans living nearby and thus some measures can only be taken once the assessment is made. This however can also be used to estimate the value of the land and related compensation for societies living in the affected area (Pivnyak et al., 2013).

In order to understand the difference between different types of mine waters, table 3 classifies them according to their mode of use, production and chemical composition. It shows the basic definitions associated with mine water, mining water, mill water, process water, a leachate, effluent, mine drainage water and in the end AMD. Mine water is naturally occurring water, which is modified by the ongoing mine operations, normally classified into surface water and subsurface water (ground water). Whereas mining water, mill water and process water are introduced by mining operations in forms of crushing the ore or containing chemicals to complete hydrometallurgical processes. AMD process generates water having very low pH often referred to as acid sulfate water (ASW) because the nature of generation, originating from oxidation of sulfide minerals explained in later sections. The differences are very important to establish the mode of their usage in literature (Lottermoser, 2010).

Table 3. Mine water definitions, with AMD highlighted (modified from Lottermoser, 2007).

Term	Definition
Type of mine water	
Mine water	Any surface water or ground water present at a mine site
Mining water	Water that had contact with any of the mine workings
Mill water	Water that is used to crush and size the ore
Process water	Water that is used to process the ore using hydrometallurgical extraction techniques; it commonly contains process chemicals
Leachate	Mine water that has percolated through or out of solid mine wastes
Effluent	Mining, mill or process water that is discharged into surface waters
Mine drainage water	Surface or ground water that actually or potentially flows from the mine site into surrounding areas
Acid mine drainage (AMD) water	Low pH surface or ground water that formed from the oxidation of sulfide minerals and that actually or potentially flows from the mine site into surrounding areas

2.2. Acid Mine Drainage

Since long, due to excavation of earth has brought up a lot of issues threatening our ecosystem. One among those is acid mine drainage threatening both surface and ground water deposits. Several mineral resources as metallic ores, like copper, silver, gold etc. are rich in sulfide and other minerals which may release harmful substances like sulfuric acid when exposed to moisture and air. The process is further accelerated by acidophilic and even eukaryotic organisms, which may control the rate at which these processes might occur. These get their energy from highly exothermic oxidation processes and the end product containing iron, aluminum, arsenic, copper, lead, zinc and manganese, being drained in surface and ground water (Jacobs, Lehr and Testa, 2014).

Pyrite weathering is the foremost cause of these acid producing processes, being one of the strongest methods occurring in nature to produce such end products (Wolkersdorfer, 2008). This is where the acid mine drainage begins at its roots carrying out the following reactions (1-4) as presented in studies (Wolkersdorfer, 2008).

$$\mathrm{FeS_2} + \frac{7}{2}\,\mathrm{O_2} + \mathrm{H_2O} \longrightarrow Fe^{2+} + 2SO_4^{2-} + 2H^+ \quad (1)$$

$$\mathrm{Fe^{2+}} + \frac{1}{4}\,\mathrm{O_2} + H^+ \longrightarrow Fe^{3+} + \frac{1}{2}\mathrm{H_2O} \quad (2)$$

$$\mathrm{Fe^{3+}} + 3\mathrm{H_2O} \longrightarrow Fe(OH)_3 + 3H^+ \quad (3)$$

$$\mathrm{FeS_2} + 14\,\mathrm{Fe^{3+}} + 8\,\mathrm{H_2O} \longrightarrow 15\,Fe^{2+} + 2SO_4^{2-} + 16H^+ \quad (4)$$

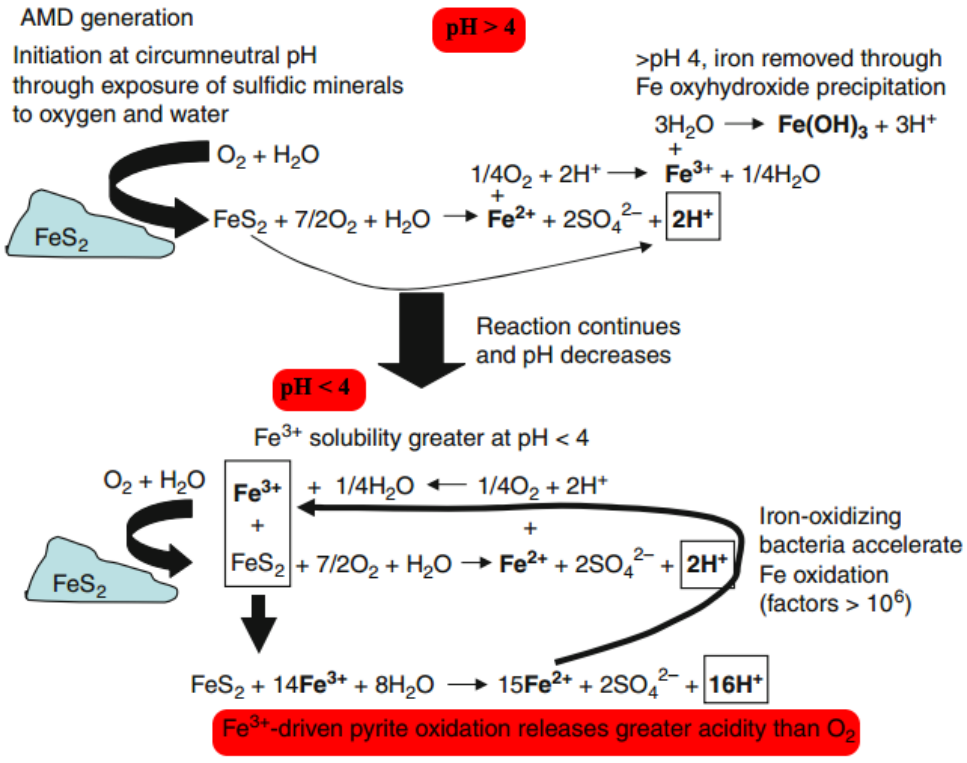

Figure 6. O_2 vs Fe^{3+}-driven pyrite oxidation resulting AMD (modified from Warren, 2011).

Table 4 shows some of the most common sources generating AMD, showing primary and some secondary sources. Apart from the primary sources, the secondary sources are normally neglected, if controlled in proper way this can be eliminated with much ease than the primary sources.

Table 4. Common sources for acid mine drainage (Modified from Akcil and Koldas, 2006).

Primary sources	**Secondary sources**
Mine rock dumps	Sludge ponds
Tailings impoundment	Rock cuts
Underground and open pit mine workings	Concentrated load-out
Natural underground water	Stockpiles
Diffused seeps	Concentrate spills along roads
Construction rocks	Emergency ponds

Mine drainage can be divided into different kinds depending on the pH, it can be listed as extremely acid mine drainage (EAMD), acid mine drainage (AMD), neutral acid mine drainage (NMD) and saline mine drainage (SD). Acid mine drainage has the pH around 1 to 6, with pH less than 1 is related to as extremely acid mine drainage.

The quantity of some metals and metalloids are higher than those set by quality standard institutes, thus causing harmful effects on living beings especially aquatic. Thus, mining activities are always subjected to complete all the necessary quality standards nowadays, as disastrous effects have been seen prior to these standards and in effect a lot mines have been abandoned. Terms such as acid ground water has been introduced because of the much worst impact on ground water as compared to surface (Lottermoser, 2007).

These sulfide minerals give away effluents and other chemical while processing, acid mine drainage may occur due to seepages in tailings impoundments where the remains of ores are dumped (Sheoran and Sheoran, 2006).

2.3. Hazardous effect of pollutants

The metal ions chosen for this study i.e. Ni^{+2}, Cu^{+2}, Zn^{+2}, Fe^{+3} are present in frequent amounts in mine generated waters and pose a serious threat to the surrounding environments, some of which is explained later. Cyanide intake on other hand is very hard to diagnose and predominantly present in mine waters. Table 5 below shows some of the hazardous heavy metal values as in maximum contamination level (MCL) set by United States Environmental Protection Agency (EPA) for drinking water quality (Barakat, 2011). These values lay the foundation of the treatment methods necessary to bring the concentrations of these elements in water to normal state.

Table 5. Hazardous heavy metals standard values and their impact on human health (Modified from Barakat, 2011).

Heavy metal	Toxicities	MCL (mg/L)
Arsenic	Skin manifestations, visceral cancers, vascular disease	0.050
Cadmium	Kidney damage, renal disorder, human carcinogen	0.01
Chromium	Headache, diarrhea, nausea, vomiting, carcinogenic	0.05
Copper	Liver damage, Wilson disease, insomnia	0.25
Nickel	Dermatitis, nausea, chronic asthma, coughing, human carcinogen	0.20
Zinc	Depression, lethargy, neurological signs and increased thirst	0.80
Lead	Damage the fetal brain, diseases of the kidneys, circulatory system, and nervous system	0.006
Mercury	Rheumatoid arthritis, and diseases of the kidneys, circulatory system, and nervous system	0.00003

These elements may find their use in essential building blocks of living beings, but the excess is however harmful in a number of ways and may even prove fatal if taken for long duration.

Zinc metallo-enzymes are crucial to neurosensory functions, immunity strength and insulin synthesis. Zinc apart from being essential for functioning of human body and present in all types of cells. It has direct and indirect influence over bone formation, tissue, brain growth. Even there is zinc deficiency worldwide affecting at least 2 billion people (Bagherani and R Smoller, 2016). It exists in form of Zn^{+2} acting as stabilizing agents for protein structures in human body, their concentration is around 2g in a normal human body (Strohfeldt-Venables, 2015).

However, the oral supplement and excessive amounts can cause skin irritations, vomiting, nausea and anemia in worst conditions if the intake is for prolonged durations, mostly associated with waters affected by AMD (Qu and Liu, 2014). Normal human intake is about 7mg d^{-1}, high contents around 24mg d^{-1} of Zn is found in meat and fish foods. Copper deficiency is directly associated with excess of Zn intake which may reduce body immunity, fetuses' death, anemia and kidney damage (Perk, 2013).

Copper has a very rich history with its mining dated around more than 2000 years ago used for production of alloys, now a days find its used in purest form for electricity networking. It has also been found essential for immunity towards several diseases, as some of enzymes in every cell of human body utilize it to carry out functions (Strohfeldt-Venables, 2015).

Apart from that copper is an important component to carry out cellular respiration, collagen synthesis and nutrient metabolism (Melzian, 2003). The suggested intake of copper is about 0.9 mg/day for adults, the intake however varies on physical condition like workout, straining and injuries. There is no or less deficiency of copper in adults, except people with genetic situation. Excess of copper however can bring certain medical conditions such as Wilson's disease in which the excess copper is accumulated in liver and nuclei of brain causing dysfunction of kidneys and brain. Too much copper can also cause iron deficiency (McPherson, Pincus and Henry, 2007). Ni and similar other contaminations are considered as carcinogenic increasing the risk of cancerous diseases. With their abilities to hinder DNA damage repair, induction of oxidative stress and inhibition of DNA methylation (Ferrante et al., 2013).

Being a ferromagnetic metal it shares chemical properties with Fe. Nickel is an essential component of certain processes in human body, but it is required in very small amounts. Excessive use however causes damage to the immune system, cell structure and chromosomes. The direct intake through food doesn't have much impact but the skin may become allergic with direct contact. Plants also suffer with Ni contamination as it affects root propagation, metabolic activities and absorption by roots, it works in a way that it replaces similar metals present in active sites in metallo-enzymes hindering their ability to work properly (Perk, 2013).

Iron accounts nearly about 5% of the earth's crust being the second most abundant metal it is found in forms of oxides, hydroxides, sulfides and carbonates mostly and not seen in its

elemental form much. It does not propose any harm to the environment or human health but due to its corrosive nature can cause corrosion in drain sewers because of presence of ferrobacteries (Lenntech.com, 2016).

Cyanide finds its use for the extraction of gold, since it replaced mercury and through 1970 has been the most dominant method to extract gold for example nearly 90% mines in Canada use cyanide for gold extraction (Eisler, 2004). The process is explained via chemical equations 5-7, first two showing the mechanism for leaching gold in form of cyanide. Gold is finally separated by reacting with zinc, which from zinc cyanide complex thus releasing Au free. Then further refined by electrolysis.

$$2\mathrm{Au} + 4NaCN + \mathrm{O_2} + 2\mathrm{H_2}O \longrightarrow 2\mathrm{NaOH} + 2\mathrm{NaAu(CN)_2} + 2\mathrm{H_2O_2} \quad (5)$$

$$2\mathrm{Au} + 4NaCN + \mathrm{O_2} + 2\mathrm{H_2O_2} \longrightarrow 2\mathrm{NaOH} + 2\mathrm{NaAu(CN)_2} \quad (6)$$

$$2\mathrm{NaAu(CN)_2} + \mathrm{Zn} \longrightarrow 2\mathrm{Au} + Na_2\mathrm{Zn(CN)_4} \quad (7)$$

For the process to be successful a huge surface area of the ore is to be exposed to cyanide containing alkaline water, may take up to 150 ha of area resulting into formation of tailing ponds which may have huge implications to the aquatic life and ecosystem since mostly the disposal mechanism for such a vast system is costly to maintain (Eisler, 2004). Spillages of these huge reservoirs for tailings have been observed as in the case (UNEP/OCHA, 2000) where 100000 cubic meters of liquid containing tailings was set loose due to a dam failure, having huge implications over the region this liquid flooded before going in the sea.

Cardiac arrest and hypotension are among the worst cases of cyanide poisoning as indicated by (Fortin et al., 2010), apart from this, low dosage may cause rhythm, conduction, and repolarization disorders. The most dangerous fact of cyanide intake is that it is hard to diagnose (Chin and Calderon, 2000).

Figure 7. Old multiferrous mine (Akcil and Koldas, 2006).

The level of contamination however depends on location and types of mining activities being carried out. Figure 7 above shows tailing pond for an abandoned mine. In past, it was a common practice to abandon the work place after mining operations without thinking of any possible drawbacks concerning AMD. Leaching of metallic ions from the mining site occurs with surface water contact with rocks because of acidity of water increased to over 10,000 times that of normal water. In general, there are two main streams to deal with AMD naming active and passive treatment, the first one involving biochemical reactions carried out in controlled environment usually without any external mechanical support. The later one some sort of assistance is needed to maintain the pH of the solution (Gaikwad, Sapkal and Sapkal, 2010).

Some technologies proposed for dealing such waste treatment are successful to a great extent while it separates wide range of elements, but if the process itself is sustainable is a big question indeed. Because the process in turn can release by products of its own in addition to the separated elements, more toxic elements are released when there is no such remedy to treat them thus making the situation more horrible (Simate and Ndlovu, 2014).

2.4. Acid Mine Drainage Treatment

Figure 8 shows the placement of water treatment facilities within an opencast mining place. With efficient design of mine workplace, the water contamination can be reduced to a great extent (Pall Corporation, 2016). Processes like reverse osmosis and membrane filtration are employed downstream of other common methods like coagulation and settling ponds. These methods have been successfully applied by Pall Corporation in Queensland Australia.

Figure 8. Water treatment setup (Modified from (Pall Corporation, 2016))

Since most of the AMD generates from waste rocks so a proper geochemical state of these needs to be made, like how effective they can be to reduce or neutralize the pH of water. Only then some acid neutralizing measures can be taken such as dissolution of carbonates (Saria, 2006). One of the measures is the net acid generation (NAG) which measures the net acid producing potential (NAPP) from the samples (Stewart, Miller and Smart, 2006).

2.4.1. Ion Exchange Method

Cation exchange method is good in targeting selective metal ions and removing them efficiently (Kilislioglu, 2015). Metal ions which contaminate waters are identified and then replaced by other ions which are not harmful and do not contribute to contamination of water. Both the exchanged and contaminating ions must be dissolved and have the same valence charge (Dąbrowski et al., 2004). The structure and size of the cation to be replaced may predict its affinity, one other factor is the type of functional group of ion. Functional groups such as –SO3H, -COOH and –OH are common in cation exchangers (Kilislioglu, 2015).

Apart from that factors such as pH adjustment, cycle length and prefilteration are of considerable importance. The resins are also needed to be selected and regenerated depending on the concentration of contamination. Regeneration can be done by removing the metallic ions using some acid during which the exchange cation is restored. Figure 9 shows the typical ion exchange flow process (ITRC, 2010). However, chemisorption shows stronger bonding as compared to cation exchange (Sheoran and Sheoran, 2006).

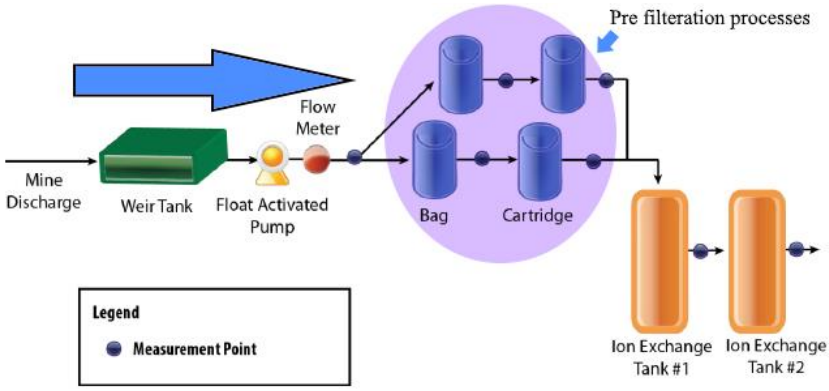

Figure 9. Ion exchange flow (Modified from (ITRC, 2010)).

2.4.2. Advanced Oxidation Processes

Mostly the reaction based on formation of OH radicals (a molecule having unpaired electron) with the help of various combinations O_3/UV, H_2O_2/UV, O_3 /H_2O_2/UV. The process is mainly used waste water treatment, drinking water supplies, gas effluent treatment, medicinal baths and

other water sanitation applications. Ozonation of water waste produces radicals, can go through direct reaction in which it directly reacts with pollutants oxidizing them. Or they can react with natural organic water to form hydroxyl radicals. In treated waste water we have a lot of organic matter, with which ozone reacts. Dissolved organic carbon and nitrite effect the ozonation process. In presence of UV light and water the O_3 breaks into O_2 and peroxide which further reacts with O_3 to form hydroxyl radicals needed for removal of organic compounds. H_2O_2 can directly be exposed to UV light wavelength range (200 to 280 nm) used to cleave the OO bond and produce hydroxyl radicals, the excess of H_2O_2 can lead to formation of HO_2 radical (Gaikwad, Sapkal and Sapkal, 2010).

For these processes to work properly the waste water must have good UV transmission. If transmission is not enough H_2O_2 and O_3 are used together to obtain the hydroxyl radicals with HO_2^- reacting O_3 often referred to as peroxone process. Ultrasound waves are employed to break chemical bonds to produce hydroxyl radicals, it is also used with other oxidation processes but being very energy intensive (Cui et al., 2014).

Photo-Fenton reaction is a 2 stage process; first one involves reaction of Fe^{+2} with hydrogen peroxide. The iron gets oxidized generating Fe^{+3} and hydroxyl radical and hydroxyl ion. In 2^{nd} step Fe^{+3} reacts with hydrogen peroxide to yield photo-reduction Fe^{+2}, H^+ which neutralized OH^- and hydroxyl radical. Thus increasing the amount of hydroxyl radical which is used to degrade waste materials.

Super critical oxidation makes use of supercritical fluid having diffusion coefficient 10-100 times to that of a normal liquid helping mass transfer with slight change in temperature and pressure causes changes in its dissolving ability. Non polar organic waste dissolves while the inorganic precipitates. The process takes place inside a reactor with controlled conditions suitable for supercritical phase.

Semiconductors find their use as photo-catalyst for waste water treatment. Some semiconductors as TiO_2 are exposed to UV light to produce a hole and electron pair, which goes onto to produce a hydroxyl radical by oxidation. A photocatalyst should be of low cost, chemically inert, no photocorrosion and not toxic. Apart from water treatment advanced

oxidation processes can purify air too, can be used for particles removal, chemicals and gases removal and removal of micro-organisms.

2.4.3. Chemical Precipitation

Chemical precipitation is a process specialized for removal of metallic cations and is the most widely used method for its removal, figure 10 general overview. The metallic ions are converted into insoluble form which is therefore easy to remove by sedimentation. In some case some sort of pre-treatment might be desirable to change the valence of ions to be removed. The solubility of these metallic precipitates is dependent of the pH, varying which they can be separated. There are several forms of precipitates depending on process are hydroxide precipitation, sulfide precipitation, cyanide precipitation and carbonate precipitation. Hydroxide precipitation is most commonly used because of relatively low costs and broad range of dissolved materials, however there is this issue of sulfate sludge which hinders the pipelines. This is effectively replaced by sulfide precipitation process because of metallic sulfides insolubility over a wide range of pH and in some cases, no pre-treatment for attaining some specific valent state is needed (Wang, Hung and Shammas, 2005).

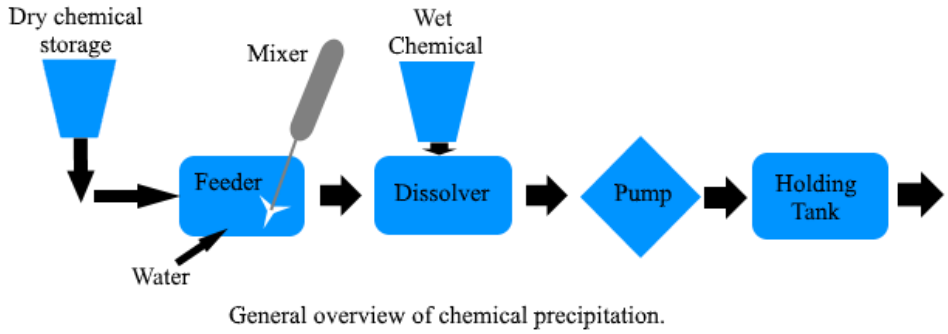

Figure 10. Chemical feed system designed for precipitation (modified from U.S. EPA, 1980).

Compared to is rivals such as ion exchange and membrane filtration the costs involved in installation and running process are quite low, but the chemical sludge produced at the end of operation needs some managing and there are costs related to that (Wang, Hung and Shammas, 2005). Table 6 shows the removal of some metal ions using lime as a base, employing hydroxide precipitation.

Table 6. Chemical precipitation metal ion removal (Fu and Wang, 2011).

Species	Initial metal conc.	Precipitant	Optimum pH	Removal efficiency (%)
Zn^{2+}	32 mg/L	CaO	9–10	99–99.3
Cu^{2+}, Zn^{2+}, Cr^{3+}, Pb^{2+}	100 mg/L	CaO	7–11	99.37–99.6
Cu^{2+}, Zn^{2+}, Pb^{2+}	0.018, 1.34, 2.3 mM	H_2S	3.0	100, >94, >92

2.4.4. Membrane Filtration

A semipermeable membrane is used to separate the input material into permeate and retentate, the former being the material which goes through the membrane and the latter is the material left behind as shown in figure 11. The driving force can be mechanical, potential difference (electrical and chemical) or temperature, upon which this process is further classified into a number of types as reverse osmosis, microfiltration, nanofiltration and ultrafilteration (Mortazavi, 2008).

Having no use of chemicals, it is a green process. Membranes can be made from polymers, metals, ceramics and liquid membranes also. The flows through a membrane are classified as dead end, cross flow and transverse flow. In dead end flow, the particles present in water are trapped in the membrane structure, in cross flow the concentrated stream helps the separated particles out, in transverse flow the water hits the membrane perpendicular, the separated water permeates from inside and the concentrate goes from outside.

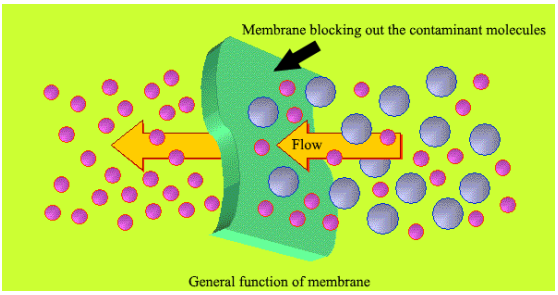

Figure 11. General membrane function (Modified from (Separationprocesses.com, 2016)).

Microfiltration can block suspended solids, and is normally the first step before nano filtration or reverse osmosis operation. Some coagulants can be used to increase the efficiency of process. Ultrafiltration on other hand can block macromolecules but still is unable to block charged particles. Main driving force is mechanical pressure for these processes, the main concerns are membrane fouling and cleaning, concentration polarization is also a problem where the contaminants too large build up near the membrane which affects the driving force and bad reactions taking place. It can be avoided by using suitable membrane, keeping concentration low and low pressure differential. Can also be used to remove iron and manganese after oxidizing and settling the minerals. A spiral wound ultrafiltration module is an innovative design in while the membrane layers are spirally wound and water pass under pressure leaving the solid particles inside while the clean water is collected upstream. Nano-filtration on other hand can block multivalent ions such as inorganic salts where the pore size is less than 2 nm, however higher pressure is needed for operation due to smaller pores resisting the flow. It employs two types of membranes, asymmetric and composite membranes, the later has options optimizing the layers separately.

Reverse osmosis, as shown in figure 12 below, is no different from other methods where water is pushed under pressure through a semi-permeable membrane, which allows some atoms or molecules to pass while others are blocked, however the driving force is concentration gradient (Separationprocesses.com, 2016). In order to desalinate the water needs to be pushed through reverse osmosis membrane by a pressure more than naturally occurring osmotic pressure, leaving around 95-99% of salts behind. Fouling of membranes is avoided because replacement is not an option for economic reasons, some techniques such as periodic pulsing of feed and filtrate, use of rotating and vibrating membrane. A more common method is to just reverse the flow pattern.

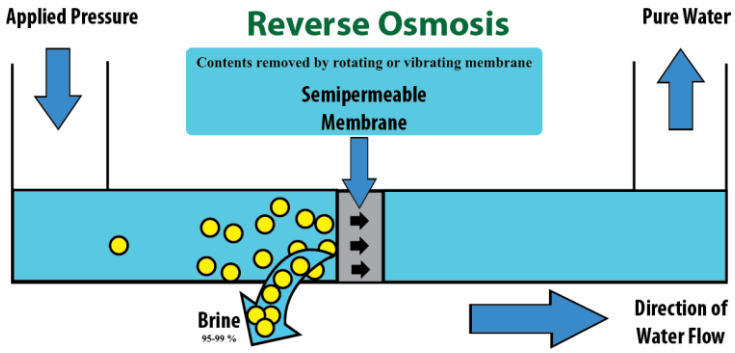

Figure 12. Reverse osmosis schematic (Modified from (Separationprocesses.com, 2016)).

2.4.5. Electrochemical water treatment

Removal of contaminants in water takes place through and electric current passed, often used with ion exchange membranes thus often called electrically regenerated ion exchange. The ion exchange membrane allows the dissolved contaminant ions to pass through it while doesn't allow water to pass. Galvanic half cells are formed with an anode and cathode. Exchange membranes are generally made by crushing ion exchange resin, adding a binder and extruding it. Different methods are employed to remove the contaminants. It operates on basic principle, applying negative charge on cathode to attract the cations which pass through a cation membrane which concentrates and leaves treated water. Electrochemical oxidation, reduction, electrocoagulation, electro deionization and electro-kinetics are some of the methods employed under this process. The reactor can be designed as packed-bed and also fluidized-bed. These methods have advantage over other methods to be able to operate at ambient temperature and pressures in addition to be able to adjust to variations in composition and flowrate.

For electrochemical oxidation the important measures are conductivity of electrolyte solution, current density, pH and pollutant concentration. The electrodes must have good stability, sufficient catalytic activity, and high oxygen evolution overpotential and resistive to corrosion. Oxidation is normally used to disinfect drinking water, industrial wastewater and odor removal from chemicals. Boron-doped diamond (BDD) electrodes show very high oxygen overpotential makes it suitable for direct contaminant oxidation, it is also referred to the adsorbed hydroxyl radical produced by electrolysis at anode. Electrocoagulation makes use of sacrificial anodes which produce metal hydroxides, these particles cause the destabilization of the pollutants when

can then be filtered easily. Current density, charge loading, pH, temperature and electrode position affect the yield of this process. Electrochemical reduction is carried out to remove metal ions which settle down in elemental forms in the end (Sharma, 2014).

Electroflotation process generates tiny hydrogen and oxygen bubbles which interact with contaminant particles making them to coagulate, these coagulates float on the water surface. The factors affecting the process are cell design, size of bubbles, electrode materials and pH. Electro-Fenton process is employed to generate H_2O_2 at the cathode, along that Fe catalyst is added used for the formation of OH radicals for the treatment of pollutants because of its strong oxidation power for organic contaminants which are otherwise hard to separate. Figure 13 shows the general overview of electrocoagulation process. The onsite production of H_2O_2 is an added advantage because the transport can be quite dangerous. Sonoelectrochemical process is combination of ultrasound and electrochemical processes, can be used with both oxidation and reduction processes. Ultrasound helps clean the electrode surface and mass transport is maximized.

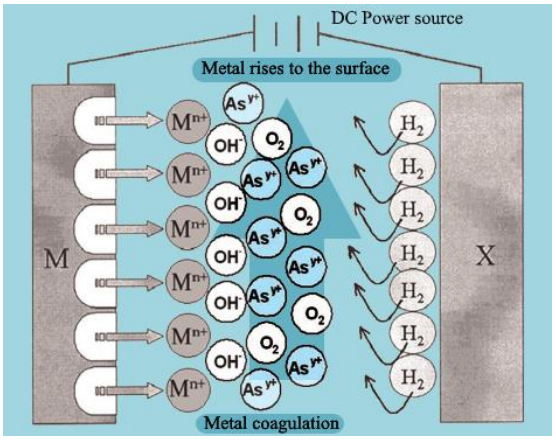

Figure 13. Layout of electrocoagulation process (modified from Sharma, 2014).

2.4.6. Biological treatment

Nowadays biological waste water treatment which exploits microbiological processes involving bacteria and other micro-organisms to break down the organic matter in the waste water are widely used in hydrometallurgical processes. Such treatment is recognized as more ecofriendly than the chemical processes. Basically the biological water treatment can be utilized in two ways such as aerobic in the presence of oxygen and anaerobic treatment in the oxygen free environment. Activated sludge is the most common example for the aerobic waste water treatment. Production of biogas from the anaerobic treatment makes anaerobic digestion processes interesting as it allows the users to benefit from it. Generally, such biological processes can be built in aquatic systems (water stabilization ponds, aerated lagoons), terrestrial systems (septic tanks, constructed wetlands operation) or mechanical systems (trickling filters, activated sludge). The choice of method for the waste water treatment depends on several factors for each process. Moreover, these biological water treatments are commonly used as secondary treatment after the primary treatment of effluents by other means. Like any other method, it has its own merits and demerits. Some of the prominent disadvantages are production of unpleasant odors, requirement of large landfill and need for sludge disposal. In order to reduce the catalytic effect of bacteria, increasing the pH may limit these organisms producing the acid (Akcil and Koldas, 2006).

2.5. Adsorption

Adsorption is a process which occurs on a solid-fluid interface, in which a substance from one phase is removed by accumulation at the interface between that particular phase and another. The material which is being accumulated or adsorbed is called solute and the material on which the adsorbate accumulates is called adsorbent. The main driving force for this sort of process is the interfacial energy of two phases, this is normally termed as surface tension accounting difference in energies as the two phases come in contact with each other as shown in figure 14.

This process is employed mostly in waste water treatment in which the toxic waste is otherwise hard to remove, the constraints on the removal of these chemicals can be the toxicity, volatility, odors, small concentrations that are otherwise difficult to trace. All these limitations are fullfiled by adsorption techniques. These toxic pollutants are mostly organic in nature, but there are a number of inorganic materials being removed as well. In these cases the pollutants are adsorbed from water and thus accumulated on another phase, thus there is no chemical reaction taking place (McKay, 1996).

Mechanism occurs in three steps, in the first step the contaminant is diffused to adsorbent surface, in the second step the contaminant moves into the pores of the adsorbent and in final step a complete monolayer is deposited. The process can be selective allowing some species to be adsorbed while others are left out, selectively removing contaminants (Worch, 2012). Adsorption can be physical and chemical depending if chemical bonds are formed or just van der Waals interaction. The adsorbate maintains their identity and the process is reversible in nature however the deposition is dependent on various parameters as specific surface area, pore shape size and volume but for chemisorption the reactivity and stability of active sites is important. Adsorbents must meet certain properties for their most effective use such as large surface area, high capacity for adsorbates, chemical and thermal stability and economically viable in terms of running costs.

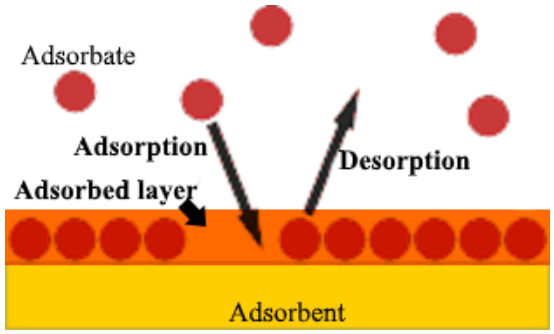

Figure 14. Schematic of adsorption process (Modified from (www2.chemie.uni-erlangen.de, 2017))

The process of adsorption is studied by means of adsorption isotherms, a plot between equilibrium concentrations of solute on surface of an adsorbent vs the concentration of solute in the liquid. The relationship however depends on the type of adsorption. There are several models for predicting the equilibrium distribution, most commonly used are Langmuir, Freundlich and BET (Brunauer, Emmet and Teller) isotherm. They can predict different types of conditions observed like monolayer adsorption, microporous materials, multilayer adsorption, porous materials and unfavorable interactions. These are mostly simple two parameter models, however if conditions are such that more complex phenomena are observed additional parameters are also introduced, however the fitting is observed with use of non-linear regression. The best model is selected on basis of apparent fit, experimental and simulated adsorption capacity and error functions. The adsorption process can be limited a number of factors for which adsorption kinetic studies are made, generally there are three steps to adsorption film transport, penetration to internal pores and adsorption to the surface site. The rate of adsorption is governed by general rate law (Worch, 2012).

2.5.1. Adsorption Isotherms

An adsorption isotherm provides an efficient means to interpret the adsorption process for the given conditions. The graph depicts the amount of adsorbate adsorbed on the surface of the adsorbent and is represented as a function of pressure under a constant temperature. In an adsorption process, the adsorbate gets adsorbed by the adsorbent through various means. There exists a state of equilibrium during the adsorption process and it would eventually shift to the direction which demonstrates a relief on the stress experienced by the system, according to Le-Chatelier principle. The influence of pressure can lead to a shift in the equilibrium direction. This shift in direction is towards the decrease in molecules and since this occurs during the forward process, the increase in pressure has a positive effect on the forward process (Worch, 2012).

Understanding the adsorbent behavior is very important for adsorber design, selection and equilibrium data. The interaction between adsorbent and adsorbate decides the equilibrium behavior, with several other factors such as individual characteristics of the adsorbent and the adsorbate along with temperature and pH of the system. In order to measure the individual capabilities of these adsorbents, mathematical models are presented, the simplest of which can be interpreted in terms of adsorbate concentration, the amount of adsorbent adsorbed and the temperature (Worch, 2012). The equation is presented in equation (5).

$$q_{eq} = f(c_{eq}, T) \tag{8}$$

Where,

q_{eq} = the adsorbed amount of adsorbent whilst at equilibrium

c_{eq} = the concentration of adsorbate

T = temperature of the system

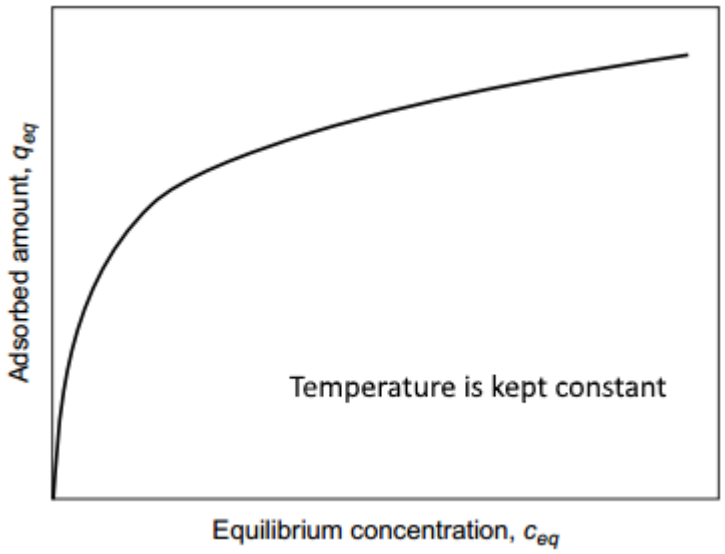

Figure 15. Example of an adsorption isotherm (modified from Worch, 2012).

The equilibrium data is measured using the bottle-point method, solution with known concentration co is taken, a known quantity of adsorbent is added to it ma. Equilibrium is established by shaking for a certain period depending on the size and shape of adsorbent particles. After shaking the equilibrium concentration is measured c_{eq}, which is used then to calculate the q_{eq}. For the calculation of the equilibrium time several parameters play their part, consisting c_{eq} and c_o ration. The general equation used is shown below where r_p is the radius of particles, D_s the diffusion coefficient and $T_{B,min}$ is the minimum time needed for equilibrium. According to the equation (6) there is a strong relation between the time required for attaining equilibrium and the radius of adsorbent particles, therefore the system is designed accordingly keeping in view the effects on equilibrium time (Worch, 2012).

$$t_{min} = (T_{B,min}\, {r_p}^2)/D_s \tag{9}$$

While most of the mathematical methods were developed for gas and vapors. Since there is no change in pressure with a liquid, however with small modifications these systems can be used for solutes as well, using the concentration instead of pressure at equilibrium state. The simplest of the one parameter isotherm system made for systems with very low concentrations is Henry

equation. This equation (7) however does not describe the larger concentration, which lead to the two-parameter isotherm among which Langmuir and Freundlich are first ones.

$$q = K_H\, c \tag{10}$$

Langmuir model (equation 8) was created in 1916 based on assumption that there is no interaction between adsorbed molecules, all adsorption sites are energetically homogeneous and there is monolayer coverage only. At very low concentrations it reverts to Henry's isotherm.

$$q = \frac{(q_m\, b\, c)}{1 + b\, c} \tag{11}$$

q_m = isotherm parameter

b = isotherm parameter

Whereas Freundluch isotherm developed in 1906 assumed that non-homogeneous energetics of adsorption sites and also accounts for multiple layers, but unlike Langmuir it does not reduce to Henry's isotherm. The more the value of K, the higher is the adsorption strength, whereas the value of n being less than one shows a favourable adsorption behavior and greater than one is considered as unfavourable (Worch, 2012).

$$q = K\, c^n \tag{12}$$

K = Isotherm parameter (adsorption strength)

n = Isotherm parameter (energetics of adsorbed sites)

However, for the gas-phase adsorption isotherms, the increase in the adsorption continues until saturation pressure P_s, beyond which the process becomes pressure independent due to the fact that there are not many available sites on the surface of the adsorbent to accommodate the adsorbate. Freundlich isotherm or Fruenlich adsorption equation establishes an empirical relationship between the isothermal variations of adsorption (by a unit mass of solid adsorbent for a fixed volume of gas) with pressure. The relation between the mass of the gas and adsorbent, x and m, and the pressure P is given by:

$$\frac{x}{m} = kP^{\frac{1}{n}} \tag{13}$$

Where k and n are adsorbent and temperature dependent constants. One major drawback of this relation is the fact that it does not yield convincing results at a higher pressure. The Langmuir adsorption isotherm is based on the proposition of the existence of a dynamic equilibrium during the adsorption process. The process is represented by:

$$A(g) + B(S) \leftrightarrow AB \tag{14}$$

Where A, B and AB denote the unadsorbed gaseous molecule, unoccupied metal surface and adsorbed gaseous molecules respectively. The general Langmuir equation which relates the number of active adsorption sites (θ) to the pressure is given by:

$$\theta = \frac{KP}{1+KP} \tag{15}$$

Where K and P are the pressure and equilibrium constant, respectively. For extreme cases involving very low and high pressures, the above equation reduces to:

Low pressure: $\theta = KP$

High pressure: $\theta = 1$

Therefore, from the above two relations, it can be understood that the Langmuir isotherm equation is valid only at low pressure. The physical importance of multilayer formation during the adsorption process was postulated by Brunauer, Emmett and Teller via the BET isotherm. For the case of Langmuir's isotherm, which is valid at low pressure, the number of gaseous molecules available on the surface of the adsorbent would be much less owing to their high thermal energy and escape velocity. On the contrary, at high pressure and low temperature, the number of gaseous molecules would increase, resulting in the case of multilayer adsorption (Worch, 2012). This is a repercussion of the increase in the thermal energy of the molecules. The phenomenon of multilayer adsorption was given by the BET equation:

$$V_{total} = \frac{V_{mono} C \left[\frac{P}{P_o}\right]}{\left[1-\frac{P}{P_o}\right]\left[1+C\left[\frac{P}{P_o}\right]- P_o\right]} \tag{16}$$

'C' is the ration between the equilibrium constants for single molecule adsorption/vacant site (K_1) and the saturated vapor liquid equilibrium (K_L). For a surface covered with unilayer gaseous molecules, V_{mono} is the adsorption volume at high pressure.

The measurement of amount gas adsorbed over a range of relative pressures at a constant temperature (typically N_2, 77 K) yields the BET adsorption isotherm curve. Desorption curves are obtained by measuring the gas removed with the reduction of pressure. Per IUPAC classification, they are classified into 6 types and the characteristics of which are explained in the following section (Figure 16).

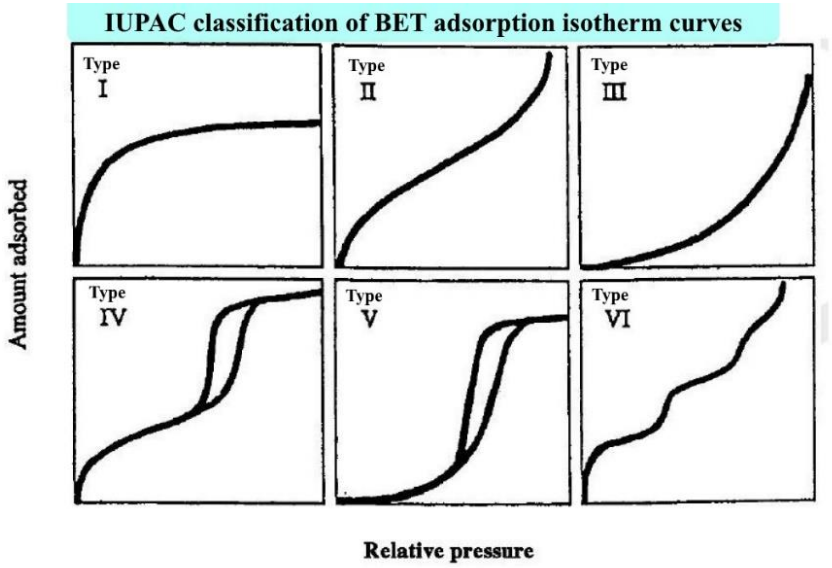

Figure 16. BET adsorption curves classification (modified from Solar et al., 2016).

Type I

The figure 16 above gives an account of Monolayer adsorption. When the pressure ratio of the BET equation is much lesser than unity and the ratio of the equilibrium constants are much larger than 1, such an isotherm is observed. A common example of such an isotherm would include N_2 or H reacting with charcoal at -1800°C. The characteristic of such an isotherm can be easily modeled using Langmuir adsorption isotherm.

Type II

Unlike type I isotherm, type II demonstrates a huge deviation from Langmuir's prediction. The intermediate region with negligible slope is an indication to monolayer formation. As in the

earlier case, the value of 'c', i.e. the ration of equilibrium constant, must be >> 1. An appropriate example of the isotherm shown in the figure 16 would be the adsorption of N_2 at -1950°C on Fe catalyst or on Silica gel.

Type III

This isotherm is capable of modelling multilayer formation in contrary to the other two types described earlier. This is evident from the fact that no part of the plot remains flat with zero slope. Such an isotherm is characteristically obtained from the BET equation with c<<1.

A typical example of such an adsorption would be the adsorption of Br_2 or I_2 on silica gel at 790°C. Also, it should be noted that the Langmuir's model is not suitable to model such an adsorption isotherm.

Type IV

This isotherm exhibits the formation of monolayer followed by multilayer at high pressure regions, similar to the type II isotherm. An appropriate depiction of such a case is seen for Benzene adsorption at 500 C on iron oxide or silica gel. The attainment of saturation level occurs below the saturation vapor pressure which is due to the condensation of gases in the tiny capillary pores even before the saturation pressure point (P_S).

Type V

This is similar to the type IV isotherm demonstrating the effect of capillary gas condensation. A prominent example of such an isotherm would be the one observed for water vapor adsorption on charcoal at a temperature of 1000°C (Solar et al., 2016).

The occurrence of hysteresis loops in the isotherm curve is due to the non-reversibility of the physisorption isotherms. Such loops can be distinguished into four types according to IUPAC classification, as shown in figure 17.

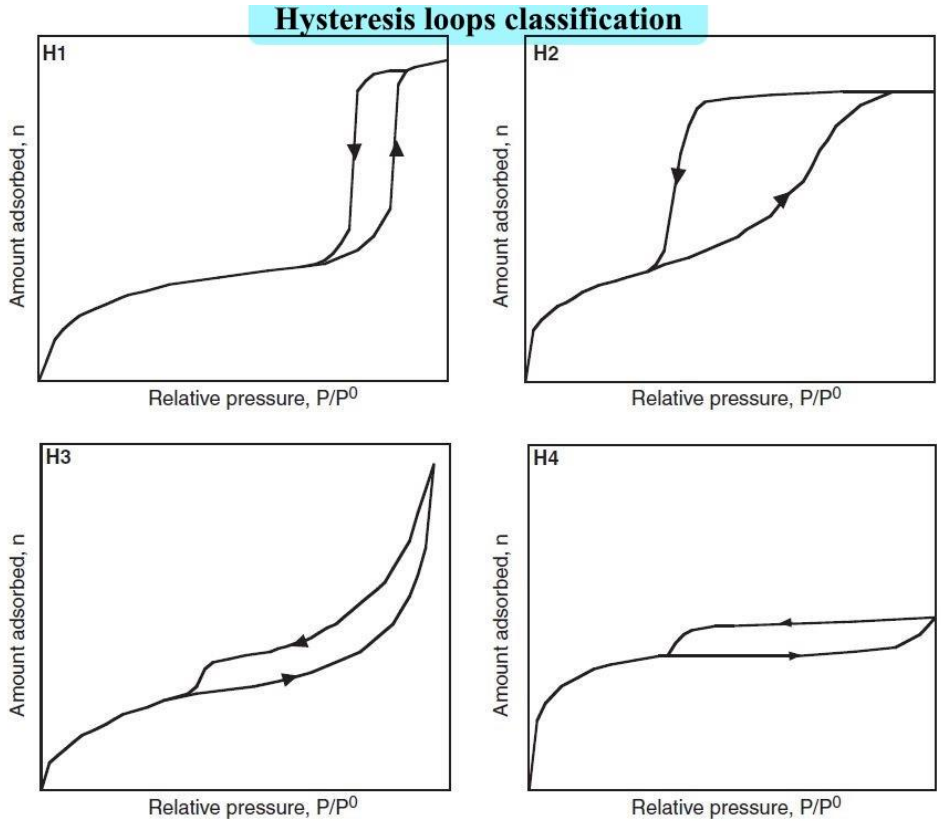

Figure 17. IUPAC classification of physiosorption isotherms (modified from Solar et al., 2016).

A distinct difference in the hysteresis loops for the adsorption of polar molecules such as water, lower alcohols, pyridine etc. with the extension of the loop over the entire pressure range is observed (Sing and Williams, 2004). This is in general the consequence of interlayer penetration and expansion/contraction of the polar molecules and clay particles, respectively (Barrer 1989). As a consequence of the activated carbons (many) and nanoporous (some) adsorbents, H4 hysteresis loops are seen with composite isotherms. In a simple process, there are two regions, an initial reversible micropore filling zone and a multilayer physisorption-condensation domain. A comparative analysis by using empirical methods the isotherm can be split into constitutive regions explaining different phenomenon (Gregg and Sing, 1982).

2.6. Adsorbents for Mine Water Treatment

For this studies we have chosen the adsorption process because of several factors including ease of access of adsorbents, rather simple operation methods and not so very complicated design (Sillanpää, 2015). The concerns related with other treatment methods are insufficient removal efficiency, which in order to cope more resources are spent. The residue bein produced can lead to secondary pollution, which is also a big concern as the process becomes not so economically viable if extra resources must be spent to tackle secondary pollutants. For more treatment methods energy and resources consumption is the main limiting factor, therefore the treatment method being proposed must be in accordance to all these limiting factors (Genz et al., 2008). The operational cost of adsorption process is comparatively very low with very little or almost no post treatment in some cases, makes it a very ideal choice. Most commonly used adsorbents are of activated carbon and alumina (figure 18), with extensive studies on modification methods to improve properties as well as iron oxide based adsorbents are quite popular as well (Tuutijärvi et al., 2009).

The selection of the adsorbents can be rather tricky, but several variables must be considered. First and foremost is the study of target ions and their potential interaction with the adsorbent molecules, this decides the removal efficiency. The process must be stable and possible formation of complex ions, but studies regarding possible formation of secondary pollutants is quite necessary too. Other thing to keep in mind while selecting adsorbents is the availability, it should be easily available. In this studies we tried to use industrial waste as our adsorbent, because of its abundance, constant production and nevertheless good adsorbent properties. The adsorption operation should be sludge free, and since the process is exothermic in nature comparatively low energy input is required (Yazdani et al., 2016).

By far many low-cost adsorbents have been studied from bio resources, industrial wastes and naturally abundant materials found making it a very reliable and cheap removal method. Modifications on these materials are continuously been made to increase the adsorbing capacities. (Cui et al., 2014) showed the potential usage of coal-based adsorbents for mine water treatment, having not so good adsorbent capacities but still economically cheap and availability

makes it a potential candidate. (Masukume, Onyango and Maree, 2014) investigated adsorption capacities of crushed sea shells in batch and column studies, the structure of the adsorbent seemed to be stable under acidic conditions. The net negative charge of clay mixtures is made to use adsorbing heavy metal ions from mine water, this has brought a lot of interest in this field (Kilislioglu, 2015). Many modifications have been proposed in recent years to increase sorption capacity. Mostly such adsorbents are used as such, with modifications being quite successful but limited by economic point of view (Worch, 2012).

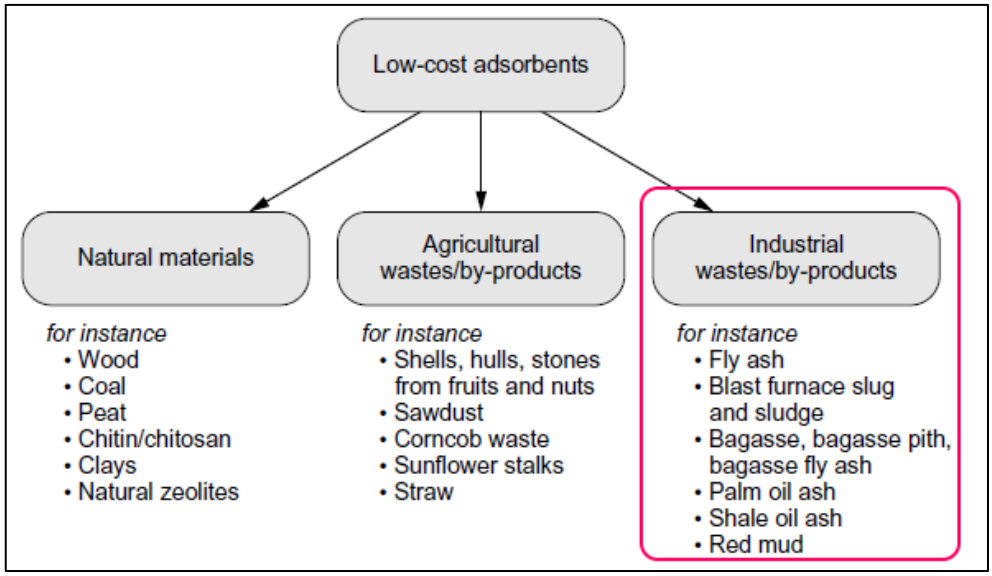

Figure 18. Some low-cost adsorbents divided by category (Modified from Worch, 2012).

Clay minerals have always been a suitable potential adsorbent for removal of metal ions from acidic nature waters. (Vhahangwele and Mugera, 2015) have reported the removal of divalent Cu, Ni, Zn, Pb and Co ions from acidic medium, the sorption affinity was found to be Cu > Co > Zn > Ni > Pb. The clay used for this purpose was bentonite achieved removal efficiency of greater than 99%. (Qu and Liu, 2014). (Xu et al., 2012) have shown some possibilities of iron oxides been used as materials for adsorption and their potential role in environment.

Industrial solid wastes have huge potential to be used as adsorbents for removal of metallic ions, especially iron containing compounds (Meng et al., 2002). (Hegazi, 2013) investigate the use of fly ash for the removal of Cu, Ni and Fe ions, since it is an industrial byproduct and its disposal is a huge concern which makes the selection of this adsorbent a positive step towards green process. Paper based industries are trying to convert the sludge produced in some of their processes, to make use as adsorbents as this study suggests (Jaria et al., 2017). Carbon based adsorbents are generated during this process by taking the sludge through a number of processes as pyrolysis and acid washing. The sludge otherwise is a useless industrial byproduct with environmental concerns.

(Iakovleva et al., 2016) studied the adsorption behavior of sulphate tailings to remove arsenic from mine water, the results found were quite compelling as compared to most commonly used activated carbon which could manage to remove just a few mg $g^{-1}$of As. Because of high iron content, high removal capacity for As was expected (Meng et al., 2002). The same study suggests the use of iron sand (RH) which also showed tendency to remove arsenic from water just as efficiently, thus laying the foundation of this study to further extend the understanding of these two adsorbents to next level, testing for the removal capability of metallic and cyanide ions from mine water. So what basically this study propose is to make use of waste generated as a result of industrial activities, treat that waste with processes as atomic layer deposition and make studies regarding water treatment.

2.7. Atomic Layer Deposition for Powder Materials

Several methods for modification of adsorbents are employed to alter its tendencies towards different environments, which is a very promising way of finding new applications for that particular adsorbent. Among these may include acid/ base treatment, microwave treatment, ozone treatment, plasma and biological modifications (Bhatnagar et al., 2013). Atomic layer deposition is a novel method and as previously conducted research (Iakovleva et al., 2016) has shown its tendencies towards removal of arsenic ions, hence chosen for this research.

Toumo Suntola modified the conventional CVD process and developed a more precise method for growing thin film structures named as Atomic layer epitaxy (ALE), which later became famous as Atomic layer deposition. The control of layer thickness is phenomenal as the process is self-timing. Lot of ongoing research is being made for the types of materials that can be deposited with this process but for now a lot of metals, metal oxides, nitrides and their sulfides can be deposited (Mastai, 2013).

The main concept of this type of deposition is that the precursors are injected in alternate manner into the reaction chamber onto the substrate provided with a purge of remaining compound after a successful pulse. Only one monolayer is chemisorbed during the pulse containing the source material, the remaining reactant is removed by an inert gas pulse. A complete molecular film is developed when the second reactant is pulsed which reacts with the monolayer developed by the first reactant. This gives a very controlled deposition of source material over the substrate, the number of repeating cycles decide the overall thickness of the layer, the main variables being temperature at which the process takes place and gas flow rate for reactants (Suntola and Simpson, 1990).

It is an alternating self-timing chemical reaction btw gas phase precursor molecules and solid substrate. Whereas the process takes place in four steps as shown below:

Chemisorption -> purge -> chemisorption -> purge

In first stage the first precursor is pulsed into the reaction chamber as shown in the figure 18 below, the molecules are chemisorbed onto the surface of the substrate making a fine layer. It is a monolayer just one molecule thick, this is why this process is called self-timing chemical reaction because of self-limiting nature of the reaction. The rest of the unreacted molecules of

first reactant are purged in the second step. The timings of exposure and the purge cycle is decided based on the temperature and the nature of substrate, normally the process is automated by formation of a recipe for the whole process. The third stage of process is the introduction of second reaction which reacts with the monolayer already formed, thus completing the chemical process to produce a monolayer of the final desired product, the remaining reactant is removed from the reaction chamber by purging at stage four.

Atomic layer deposition (ALD) was selected for this studies because of the uniformness of the layer deposited by this process being important for the adsorption process. With the ability to coat very precisely to 50 nm, ALD gives this unparallel uniformity. Compared to conventional CVD process, ALD has following advantages (Sundew Technologies, Llp, 2017).

- The process continues layer by layer whereas in CVD it is continuous, i.e. on a given point the thickness migh differ from any other point.
- The rate of layer development can be calculating with very precise results whereas in CVD the growth is not dependent on the number of cycles but is proportional to the design of the process.
- The number of cycles for all the stages, will reflect the total thickness just as predicted by the growth rate.
- The layer formed has very low or negligible internal stresses, giving it structural stability whereas in CVD there might emerge some compressive stresses which sometimes may appear in from of cracks and pinholes.

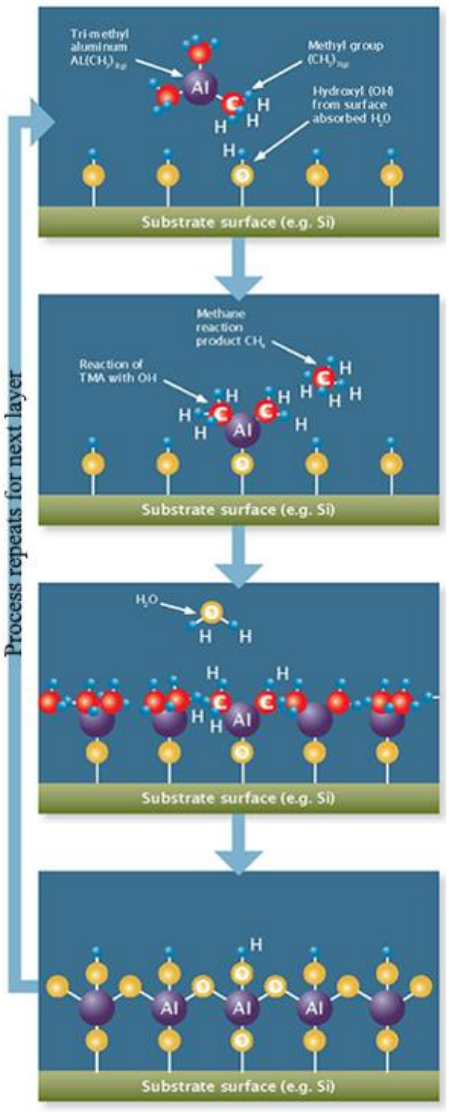

Figure 19. Steps involved in ALD process (Modified from (Ultratech/CNT, 2017)).

3. MATERIALS AND METHODS

3.1. Materials and Chemicals

The first adsorbent used was industrial solid waste by name of RH, since its good performance in prior studies with removal of arsenic ions from mine water (Iakovleva et al., 2016). Hence it is utilized with ALD modifications by depositing Al_2O_3 and TiO_2 layers. It was utilized to treat Ni, Cu, Fe, Zn and SO_4 ions from mine water. For this purpose, it is milled to 0.2 mm particle size, these particles are then washed and put to drying for 12 hours at 80°C. Table 7 shows the composition of RH as shown through XRF and XRD analysis. This adsorbent was used to treat both real and synthetic AMD.

Table 7. Chemical composition of RH (Iakovleva et al., under review).

Elements	wt %
Si	0.2
S	17.6
K	0.3
Ca	14.4
Ti	2.3
Mn	0.27
Fe	7.2
Gypsum $Ca(CO_3)$	

The real AMD was obtained from sulfide mine and depth of 720m, table shows the chemical composition of the real AMD. Electric conductivity, pH and oxidation reduction potential were measured on site. The main ions this study tends to remove were 4.41 mg L^{-1} of Cu^{+2}, 242 of mg L^{-1} Zn^{+2}, 52.6 mg L^{-1} of Fe^{+2}, 8.1 mg L^{-1} of Ni^{+2} and 3470 mg L^{-1} of sulfate ions.

Table 8. Chemical composition of real AMD (Iakovleva et al., under review).

Level	Cu^{+2}	Zn^{+2}	Fe^{+2}	Ni^{+2}	SO_4^{-2}	Redox	pH	Cond.
m	mg L^{-1}	mg L^{-1}	mg L^{-1}	mg L^{-1}	mg L^{-1}	E		ms m^{-1}
720	4.41	242	52.6	8.1	3470	422	3.2	481

Synthetic AMD was prepared using Milli-Q ultrapure water, known amount of $FeSO_4.5H_2O$, $CuSO_4.5H_2O$, $ZnSO_4.7H_2O$ and $NiSO_4.6H_2O$ are added to prepare 1g/L solution of each Ni, Cu, Fe, Zn and SO_4 ions, which were further diluted to 200ppm. 40ml of solutions are mixed with 400mg of the adsorbents prepared and checked for removal efficiencies separately for each ion.

Figure 20. Preparation of 1gL^{-1} of synthetic AMD.

Two solid wastes, as adsorbents CaFe- Cake and SuFe, by Norilsk Nickel Harjavalta, Finland were also used. There were sulfate tailings being produced as wastes in metal extraction processes and were being tested with some ALD modification depositing Al_2O_3 and TiO_2 for removal of cyanide from synthetic mine water. The materials were grounded and dried for 12 hours at 60°C. For the granulation of both these materials polyvinyl acetate (PVAc) was used,

the dissolving process was carried out with acetone as a solvent for binder obtained from Merck UK. This mixture is stirred for 20 minutes at 60°C for increasing homogeneity. Granules of the materials are then prepared using high shear granulator, Kenwood KM070 Japan. First the mixture is mixed without the binder, the amount of CaFe and SuFe added separately was 150g, mixed for 60 seconds. The impeller speed maintained was around 220 rpm and the binder was added to the powder, after which the mixing took place for about 2 minutes until granules are formed.

Table 9 shows the binder solution viscosity as a function of concentration of PVA been added, the concentration varied was from 10% wt to 40% wt. Haake VIscotester C was used to determine the viscosity of binder solution.

Table 9. Viscosity of binder solution with varying PVA (Haake Viscotester C).

C_{PVA}, %	μ, mPa·c
10	1.4
15	13
20	37
25	52
30	72
35	111
40	157

Table 10 shows the composition of CaFe and SuFe tailings showing some fair amount of Fe in both tailings, 10% in case of CaFe and around 39% in SuFe, as Fe oxides and hydroxides are found to be efficient adsorbents for removal of many contaminants through ion exchange. The precursors used to carry out atomic layer deposition process were obtained from Volatec Ltd, Finland.

Table 10. Chemical composition of SuFe and CaFe (Iakovleva et al., under review).

Elements	CaFe-Cake, wt %	SuFe, wt %
Si	<2	<3
K	0.025	0.026
Ca	11.9	0.16
Fe	10.0	38.7
Specific surface area, $m^2\ g^{-1}$	6.5	12.3
Volume adsorbed, $cm^3\ g^{-1}$	0.02	1.2
Pore size, μm	0.55	0.9

3.2. Synthesis

For deposition of Al_2O_3, trimethyl aluminium $Al(CH_3)_3$ (TMA) was utilized and titanium tetrachloride $TiCl_4$ (TTC) was utilized for depositing TiO_2 layer on the adsorbents. Two instruments from BENEQ Oy, Finland were used for the deposition, TFS 500 and TFS 200. Single chamber reactors were used with alternate pulses of TMA and H_2O precursors. The pulse and purge timings were optimized based on series of study on the depositions made. The thickness of layers developed was controlled by placing silicon wafers. In the end of process, the deposition was judged by physical examination and by means of spectroscopic ellipsometer (J. A. Woollam Co. Inc. USA). The rate of deposition was judged by taking average of a number of samples. The deposition on the powder and granules samples was confirmed by XRD analysis where several peaks were observed corresponding to respective oxides.

The deposition was carried out in single chamber reactor for TFS 500 (figure 18). The cycles were limited to 500 to get an approximate metal oxide layer of 50nm. The deposition rate was approximated for both the deposition process and estimated to be 1.1 Å/cycle for Al_2O_3 and 0.628 Å/cycle TiO_2, an average for 5 readings for both Al_2O_3 and TiO_2 was taken in order to get the rates. This was done by placing monocrystalline silicon wafers inside the reaction chamber along the powders, the end products were evaluated using spectroscopic ellipsometer.

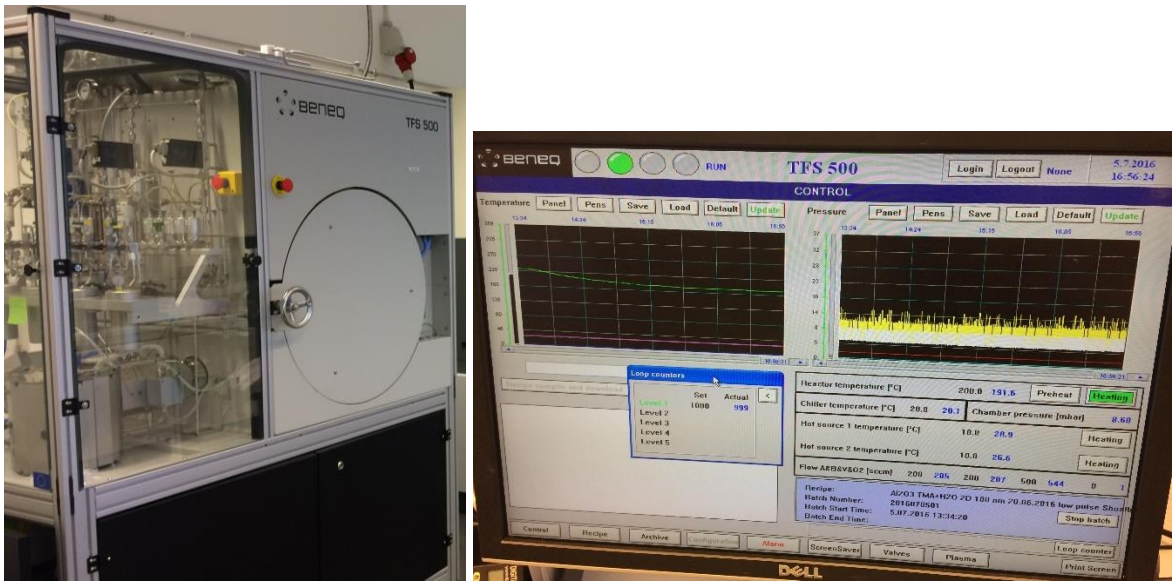

Figure 21. BENEQ TFS 500 equipment for ALD (left), Control window for process (right).

The process schematic is shown in the figure 18, showing the step by step process. In first step the trimethyl aluminum is pulsed developing monolayer onto the substrate surface, the remaining molecules are purged by a neutral carrier gas. In third step water is pulsed into the reaction chamber reacting with the monolayer formed in first step, to complete the overall reaction depositing monolayer of Al_2O_3 onto the substrate surface. The parameters for the deposition process are shown in table 12.

Table 11. Parameters for deposition of TiO_2 and Al_2O_3 (Iakovleva et al., under review).

	TiO_2 deposition		**Al_2O_3 deposition**	
Precursors	$TiCl_4$	H_2O	TMA	H_2O
Pulse time, sec	0.6	0.25	1.2	2
T ºC	350		220	
Pressure, mbar	6.5	6.5	6.5	6.5
Cycles amount	500		500	

A recipe is prepared in the control software (figure 18) to change the parameters for the process. Separate recipes are prepared for different materials, changing the pulse time, purge time, temperature, feeding pressures for the precursors and the number of cycles for which the process is carried out. Depositions on powder materials has not been studied much, so optimizing the process for powder samples was a concern, for that a number of experiments were performed to get complete deposition. Deposition rates are also function of temperature and feeding pressure, so silicon wafers were placed in the reaction chamber for controlled deposition. The wafers were continuously checked with ellipsometer to keep check on layer thickness. Figure 19 shows the number of steps involved in Al_2O_3 deposition process.

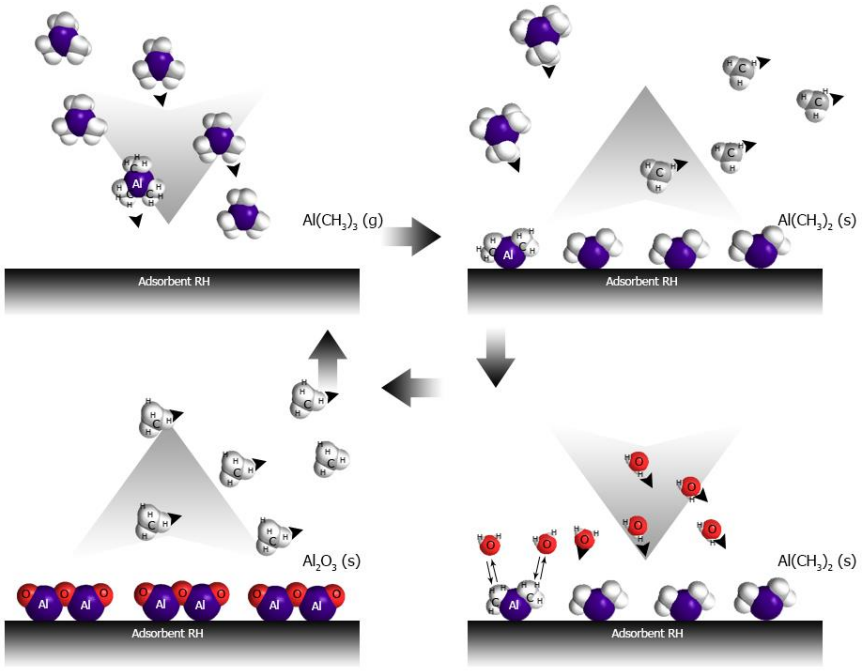

Figure 22. Schematic of deposition of Al_2O_3 onto the substrate (Iakovleva et al., under review).

3.3. Characterization

The morphology of the deposited aluminum and titanium oxides on raw materials was determined by scanning electron microscope (SEM, Nova Nano SEM 200, FEI) along with chemical composition energy dispersive spectroscopic (EDS) analysis. The materials were sputtered with gold layer and the process carried out in secondary electron mode and low vacuum less than 2 Torr. The topology of the modified and unmodified samples was realized using atomic force microscopy (AFM, Park NX10, Park Systems). this also gave the idea of approximate size of the powder particles.

The chemical composition of all the materials was confirmed with X-Ray flourescence (XRF) sepectrometric analyser X-Art (Joint Stock Company Comita, St. Petersburg, Russia) based on Si(Li) detector capable of detecing chemical elements in range from Mg to Pb (Serebryakov et al., 2004).

X-Ray diffraction patterns were observed using PANalytical Empyrean powder diffractometer using Co Kα reflection mode, the divergence slit and Ni-filter used, the process was performed over 2Θ range of 10-80° with a step size of 0.007° at atmospheric pressure and temperature. Expert Highscore application was used to analyze the diffraction patterns and possible determination of peaks.

To detect the active functional groups on modified and non modified samples FTIR was utilized. Fourier transform infrared spectroscopy (FTIR) was conducted with Bruker Vertex 70v equipped with DLaTGS detector cover a wide spectral range 12000 to 250 cm^{-1}. The measurements were made in mid infrared region 4000-350 cm^{-1}.

J. A. Woollam M-2000UI spectroscopic ellipsometer was used to measure the thickness of the deposited layers by placing silicon wafers along the powder raw materials to keep a check on thickness. For silicon wafers, Si model was used for the substrate with a thickness of 1mm and Cauchy model was used to approximate the thickness of the deposited layers of Al_2O_3 and TiO_2.

Zeta potential of the samples was measured using Zetasizer nano (Malvern Instruments Ltd).

3.4. Batch adsorption experiments

Two separate experiments were carried out, one for removal of metallic ions from real and synthetic AMD, second experiment to remove cyanide from synthetic mine water. Batch adsorption tests for first adsorbent was carried out by mixing RH in 45 mL of synthetic AMD solution prepared with known ion concentration. Mechanical shaker (CAT M.Zipper GmbH, Staufen, Germany) was employed to mix the samples for time intervals between 30 mins to 24 hours. A 0.2 micrometer polypropylene syringe filter was used for filtration of samples taken after several intervals of time. Filtrates were then analyzed for pH and ion concentration. Inductively coupled plasma optical emission spectroscopy (ICP OES) was used to determine the concentration of Cu^{2+}, Zn^{2+}, Ni^{2+} and Fe^{3+} metal contaminant ions in the solution.

Concentration of sulfate ions in the solution was confirmed by high performance liquid chromatography (HPLC), for which 2ml samples were taken from the solutions and filtered. The equipment used was a Shimadzu HPLC (Model CDD-10A; column: 4.0 mm ID × 250 mmL Shodex IC SI-50 4E; mobile phase: solution of 3.2 mM Na_2CO_3 and 1 mM $NaHCO_3$ in ultrapure water; flow rate: 0.7 ml/min; temperature: ambient).

Experiments with removal of cyanides were performed by preparing 15mL of synthetic solution of potassium cyanide (MERCK, Germany), approximately 0.5 – 40g/L of adsorbents CaFe and SuFe were mixed and shaked for interval 1 to 720 hours. 1.5 mL of the samples were taken from the solution and filtered using 0.2 um polypropylene syringe filters. However a different setup was used to evalutate the concentraion of cyanide ions, same Shimadzu HPLC was used with (column: 6.0 mm IDx250 mm L Shodex RSpak KC-811; eluent: solution of 1 mM H_2SO_4 in ultrapure water; flow rate: 1.0 mL/min; temperature: 40 ^oC; reagent 1: 0.1% Chloramine T in 0.1 M phosphate buffer (pH 7.5); reagent 1 flow rate: 0.5 mL/min; reagent 2: 1-Phenyl-3-methyl-5-pyrazolone + 4-pyridinecarboxylate (Na); reaction temperature: 80 ^oC; wavelength: 638 nm).

Following formula was used to calculate the percentage adsorption:

$$Ads\ \% = \frac{C_i - C_t}{C_i} \cdot 100 \qquad (17)$$

In this equation C_i is initial concentration and C_t is the final concentration after adsorption.

4. RESULTS AND DISCUSSION

4.1. Characterization

FTIR was performed to check the variation caused by the ALD modification by Al_2O_3 and TiO_2 for modified and unmodified RH material. With the unmodified RH the most distinct peaks observed were for following; O-S-O around 1120-1160 cm^{-1}, Si-O-Si around 660-661 cm^{-1}, O-Si-O around 466-473 cm^{-1} and H-O-H around 1620-1690 cm^{-1}. The sulfur sites present on the unmodified RH are a concern because it might cause secondary pollution during the desorption process (Iakovleva et al., 2016).

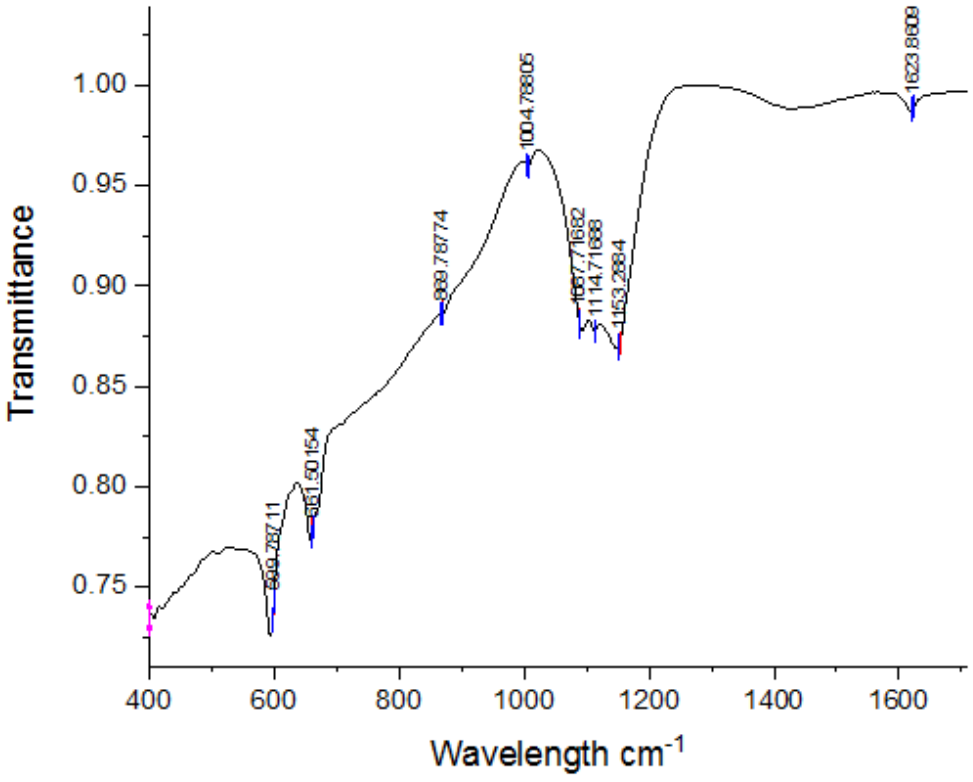

Figure 23. FTIR spectra of unmodified RH.

In RH deposited with Al_2O_3, some bending vibrations corresponding to Al-O were observed around 980-100 cm^{-1}. O-Al-O vibrations were observed around 610-611 cm^{-1}. Interesting observation was made that the active sulfur sites were not observed in the modified samples which might have caused secondary pollution, for both the Al_2O_3 and TiO_2 modified samples. the rest peaks observed were same as that of the original material apart from the fact that no peak observed around 1120-1160.

The FTIR spectra of TiO_2 modified RH observed some peaks around 450 to 800 cm^{-1} (Iakovleva et al., 2016) indicating the bending vibration for O-Ti-O, the rest peaks observed were same as that of the original material.

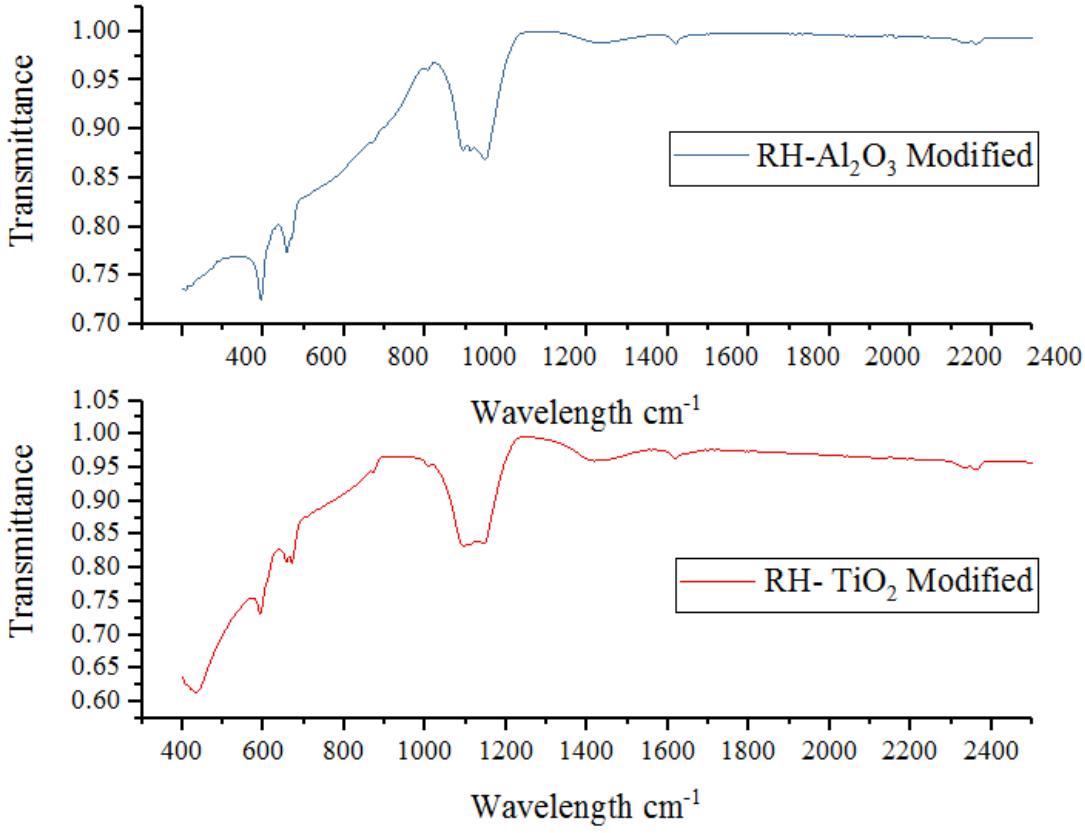

Figure 24. FTIR spectra of Modified RH, Al_2O_3 modified above and TiO_2 modified below.

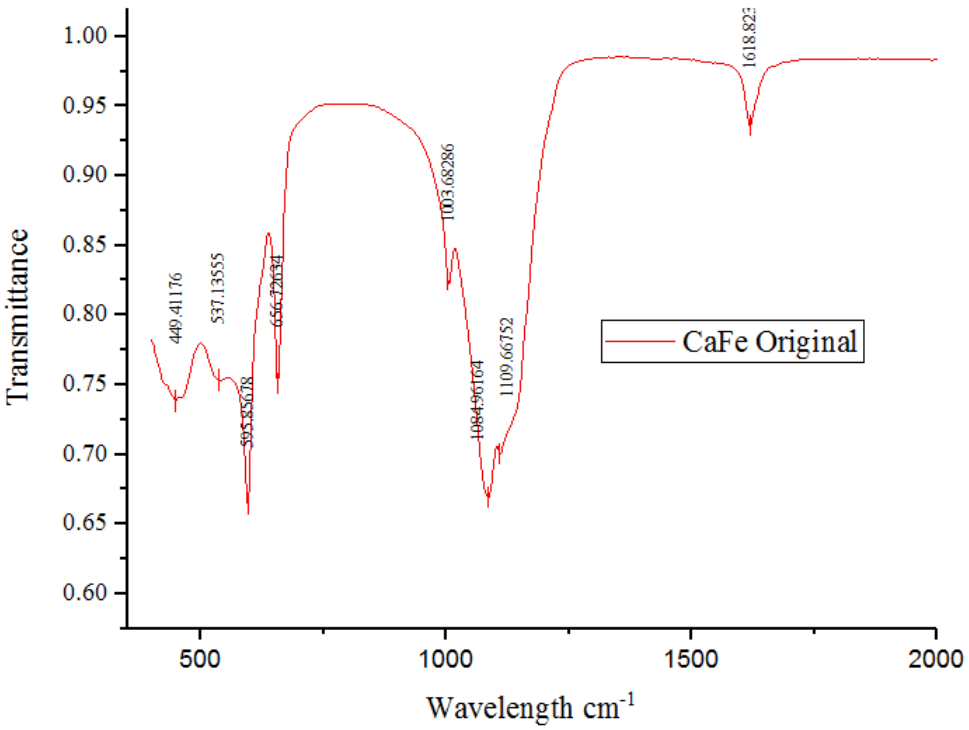

Figure 25. FTIR spectrum for CaFe original.

The FTIR spectra of unmodified and modified CaFe are depicted in Figure 22 and 23. According to the literature, the bands observed at 661-600 cm^{-1} and 473-466 cm^{-1} are characteristic of bending vibration of Si-O-Si and O-Si-O respectively (Sitarz, 2008). The bands obtained at 1620-1690 cm^{-1} and 3407-3610 cm^{-1} are assigned to the adsorbed water, either by physical or chemical means. The range from 3300 to 3600 cm^{-1} are usually reported to the hydroxyl terminals or H-bonded water and the band at 1600 cm^{-1} are a contribution to the scissor bending vibration of the water (Beganskiene et al., 2004). Additional bands at 3406-3407 cm^{-1} appeared only at the spectra of adsorbents modified with NaOH which could be the result of new bending vibration of H-O-H. The spectra from the modified adsorbents shows that the band occurring at 800-450 cm^{-1} is due to the presence of TiO_2 which indicates the TiO_2 layer deposition onto the bare CaFe cake. On the other hand, Al_2O_3 deposition can be confirmed from the bands recorded at 980-1000 cm^{-1} (Al-O stretching bands) and 611 cm^{-1} (Al-O_2 bending vibration).

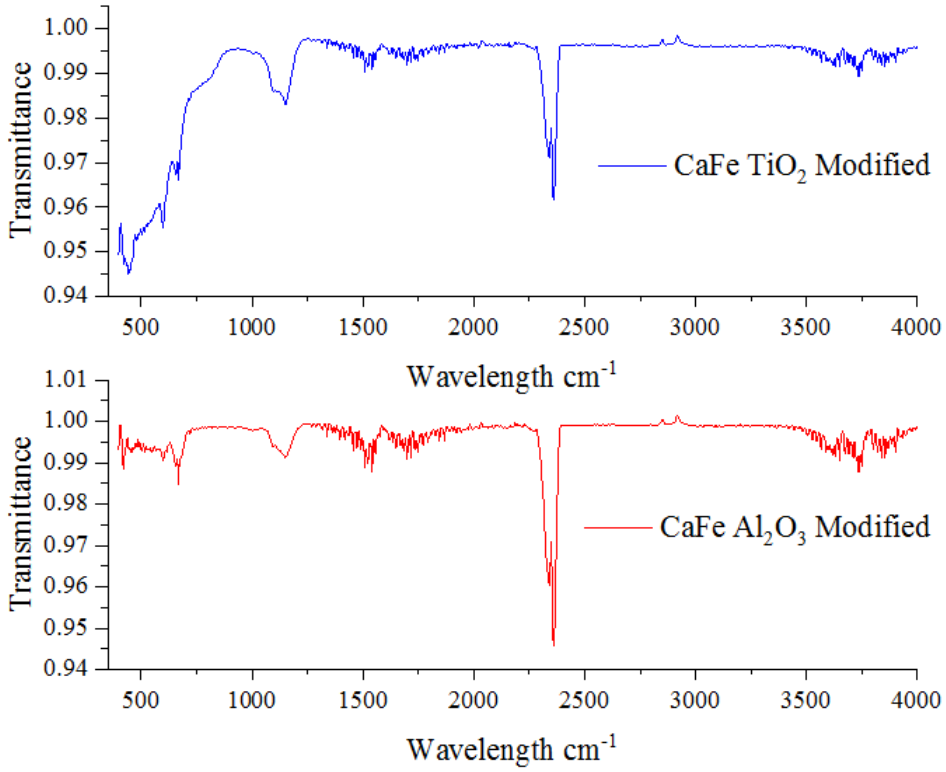

Figure 26. Modified CaFe FTIR spectra.

The graphs shown in Figure 24 illustrates the FTIR transmittance spectra for the SuFe adsorbents before and after modification with Al_2O_3 and TiO_2. As elaborated in the previous paragraph with CaFe adsorbents, the peaks near 450 cm^{-1}, 660 cm^{-1}, 1100 cm^{-1} are related to the fundamental Si bonds. They can be attributed to the rocking mode, bending vibration of Si-O-Si and asymmetric vibration of Si-O respectively (Beganskiene et al., 2004). Like CaFe spectra, the bands over the domain around 800-450 cm^{-1} and 980-1000 cm^{-1} are harvested from the deposition of TiO_2 and Al_2O_3 respectively, after the ALD process. This confirms the deposition of Al_2O_3 and TiO_2 onto the SuFe cakes. From the overall inspection and thorough interpretation of the FTIR spectra for all the adsorbents (RH, CaFe and SuFe) before and after modification with the ALD process, the Al_2O_3 and TiO_2 deposition could be found through the above-mentioned findings.

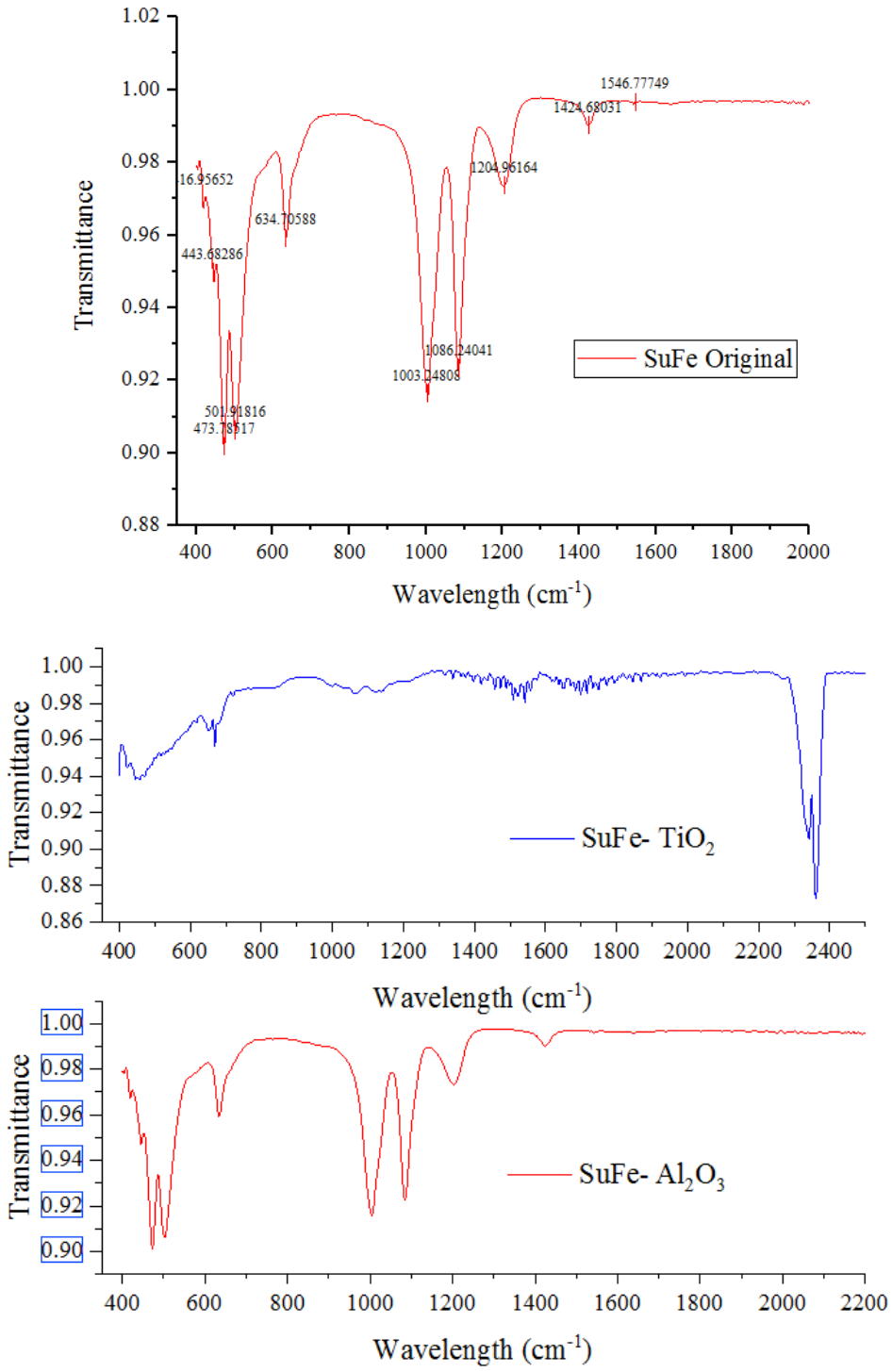

Figure 27. FTIR spectra of SuFe Original (top), SuFe_TiO_2 (middle) and SuFe_Al_2O_3 (bottom).

With the modification of RH with metallic oxides changed the surface morphology of the samples, as observed by scanning electron microscopy, as shown in figure 25a the original RH in contrast to the modified materials Figures 25b and 25c showing modified TiO_2 and Al_2O_3 respectively. The magnification used was 49.31k, 49.69k and 101.39k respectively. The porosity on the surface increased as fine pores can be observed in modified samples, as the porosimeter data confirms the pore size of both materials is reduced to 3 nm and 20 nm respectively, as opposed to the original material having 180 nm. It is quite evident from the images that the RH_TiO_2 surface area has increased to about 125 m^2g^{-1}, as shown by BET results, double as compared to the original material, similar is for RH_Al_2O_3.

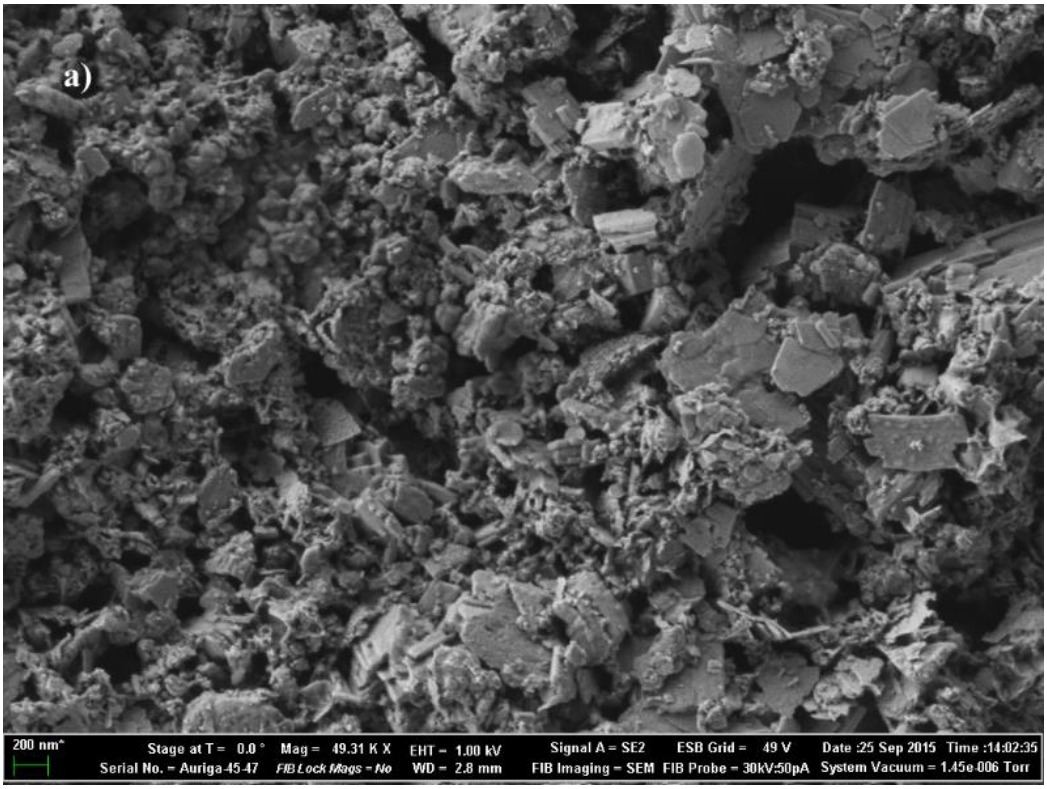

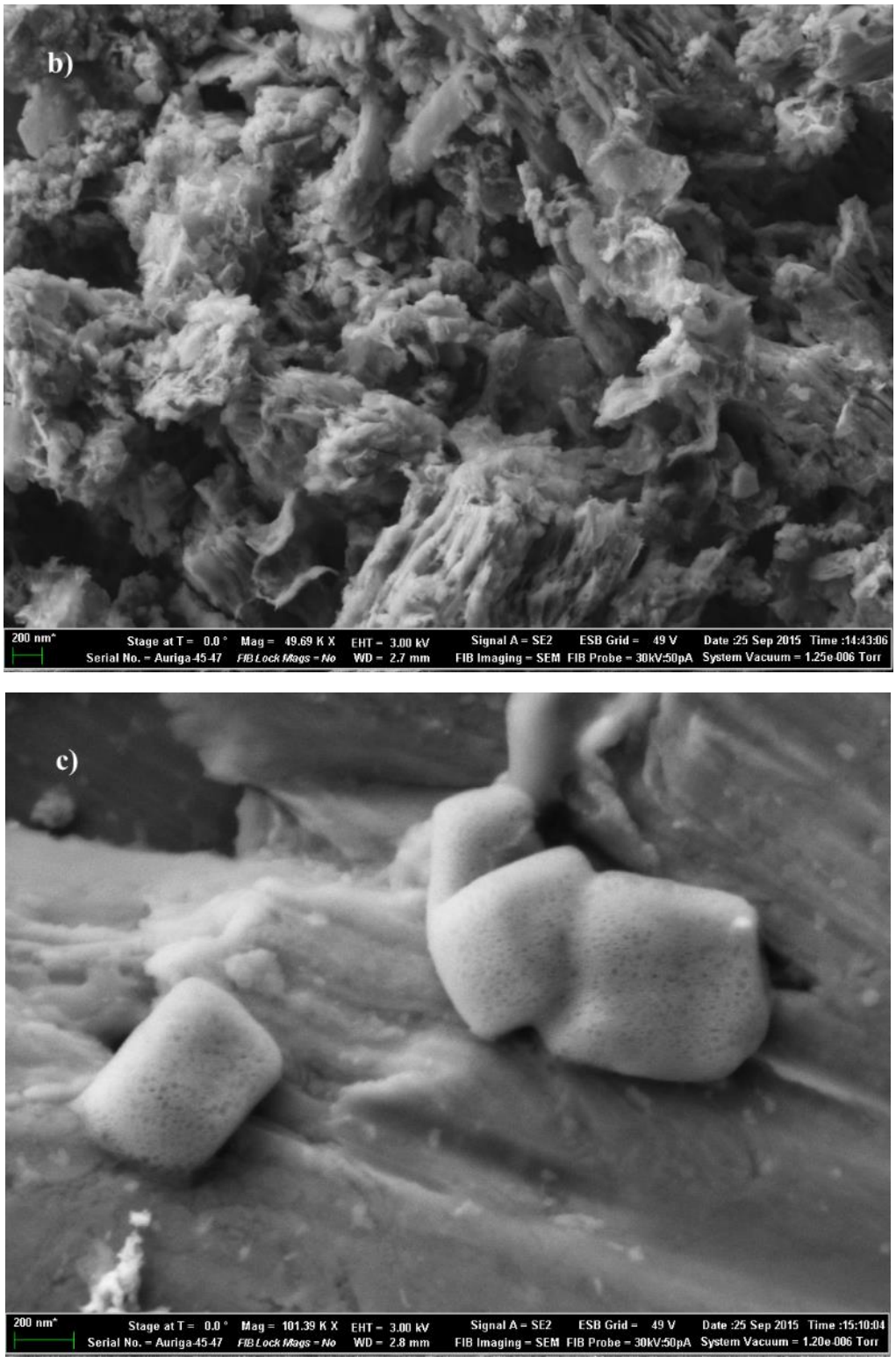

Figure 28. SEM images of unmodified and modified RH samples; a) RH_Original, b) RH_TiO_2 and RH_Al_2O_3 (Iakovleva et al., under review)

AFM results were taken in order to see the surface topography for the samples, it is quite hard to gather information regarding the porosity due to sample preparation limitations for AFM, however it is quite evident to approximate the particles size, for that small amounts of materials were sonicated for 20 minutes in ethanol and then dried at room temperature. For some samples such as RH_Al_2O_3 (figure 26b), the separation of particles from agglomerates was quite difficult and not much information gained from analysis. In figure 27 we can see before and after coating images for CaFe and SuFe materials, the surface seems to be having more surface area after the deposition process.

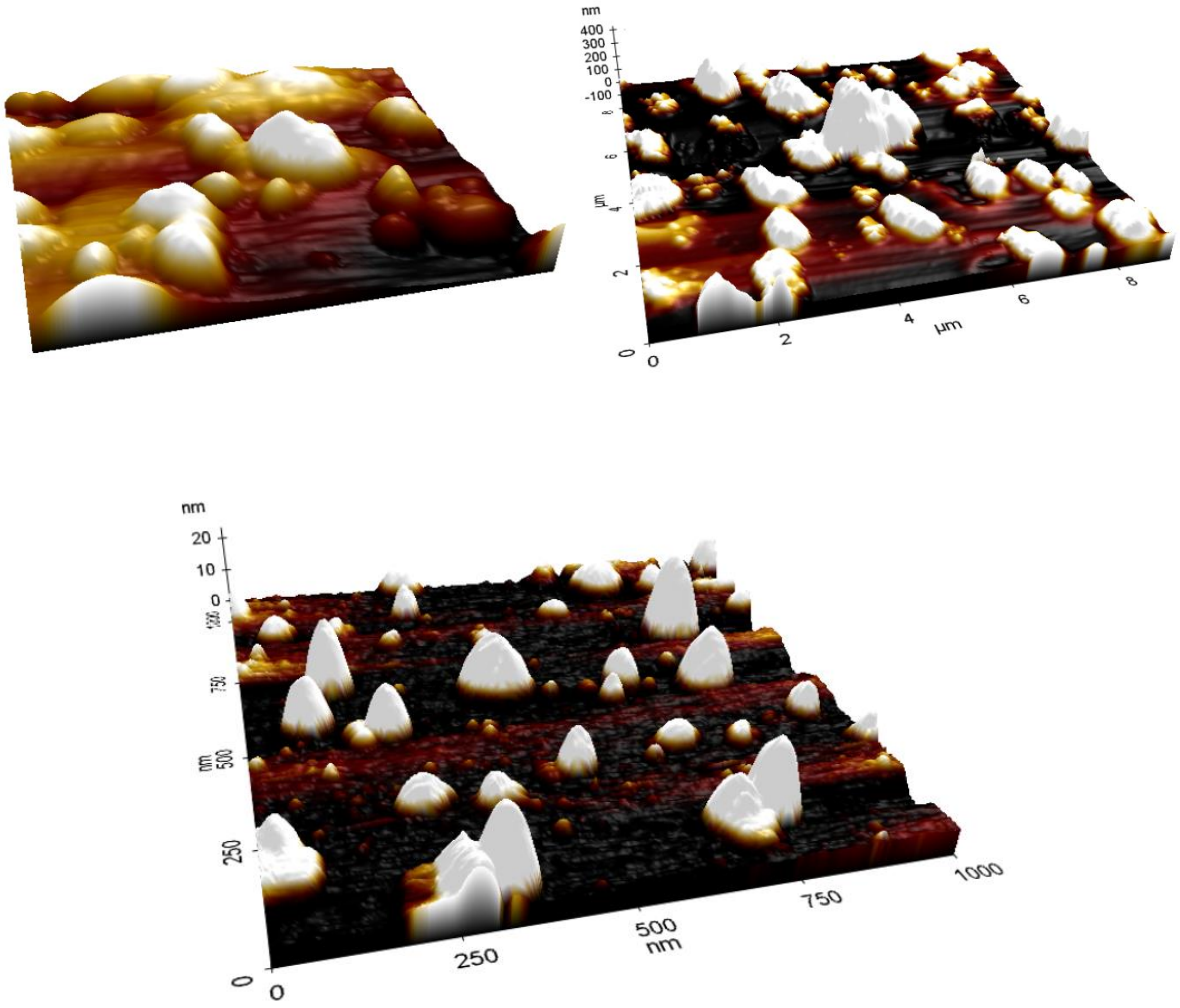

Figure 29. AFM images for original RH (top left), RH_Al_2O_3 (top right) and RH_TiO_2 (bottom) samples.

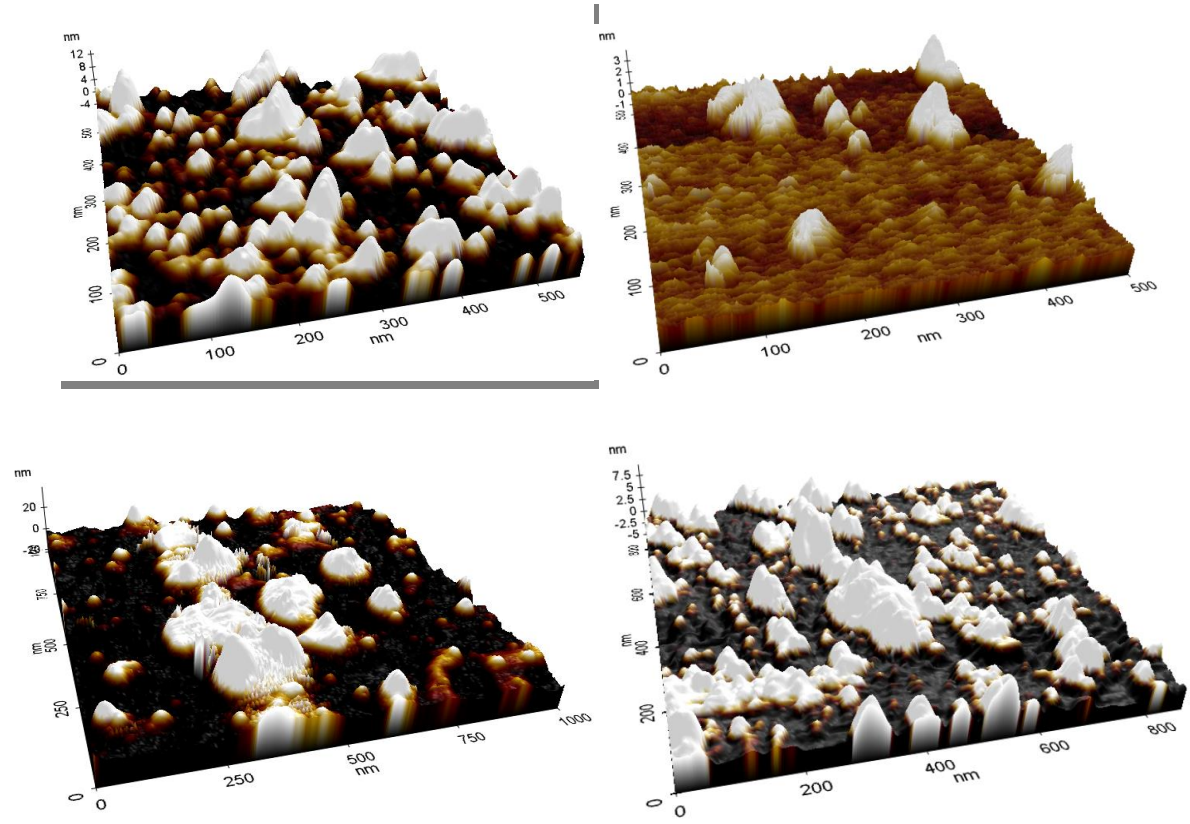

Figure 30. AFM images for original and modified materials, a) SuFe_Original, b) SuFe_Al_2O_3, c) CaFe_Original, d) CaFe_Al_2O_3.

X-Ray diffraction patterns were obtained in order to confirm the presence of phases expected from the atomic layer deposition into the samples. Original material for RH shows peak matching for gypsum $CaSO_4.2H_2O$, with the peak intensities of [0 2 0] and [0 2 -1] being quite prominent. Antase phase of TiO_2 was confirmed with the presence of [0 1 1] being the dominant peak but [0 2 0] orientation was also found. For Al_2O_3 modified sample the dominating peak was [0 1 1] with [0 1 3] and [1 2 2]. The phase was identified as Alumina Al_2O_3 Kappa, the remaining peaks were consistent with the original material.

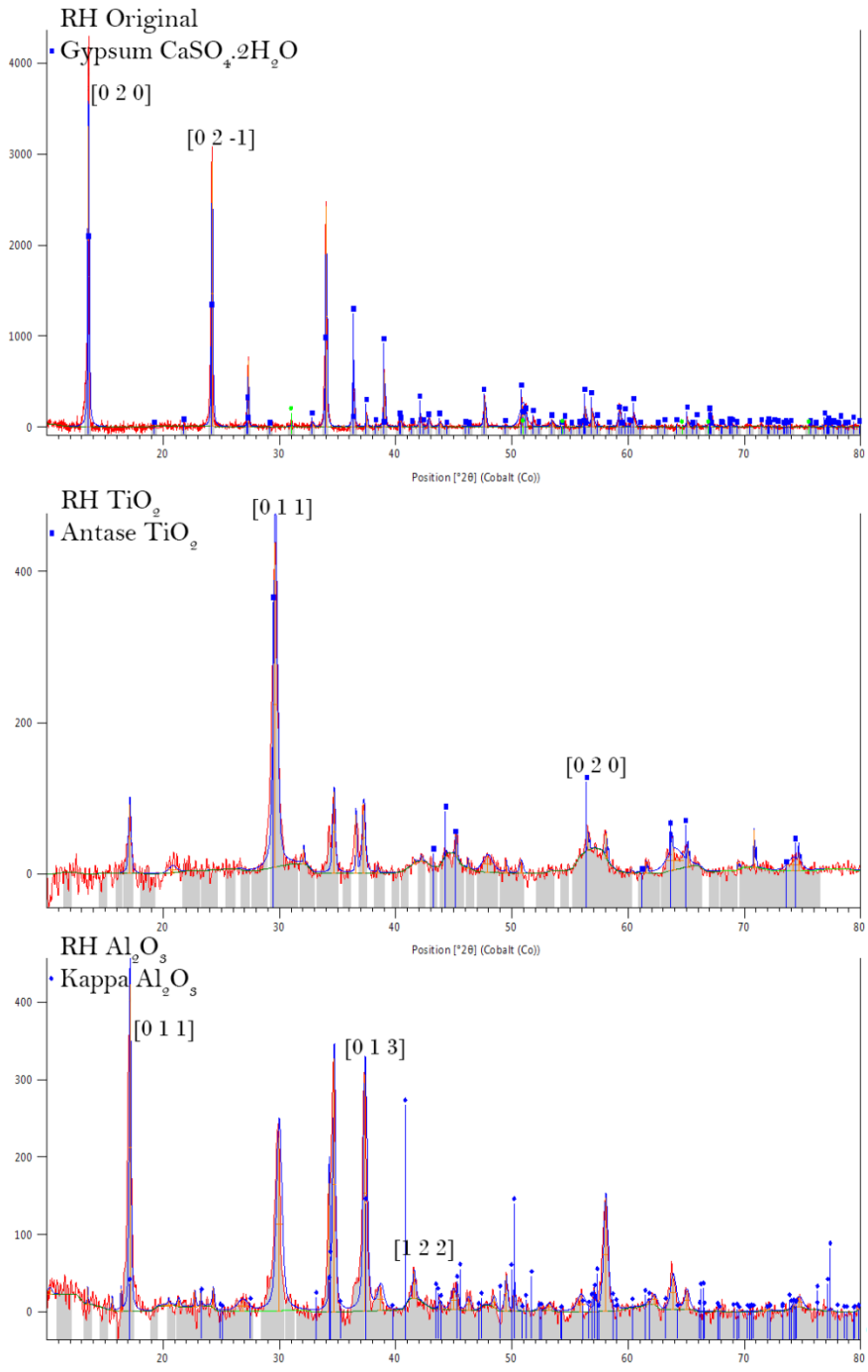

Figure 31. XRD patterns for RH, RH_TiO_2 and RH_Al_2O_3 (Iakovleva et al., under review).

The XRD patterns for the modified SuFe and CaFe samples didntot show any peaks for Al_2O_3, this can be because of amorphous nature of the deposited layer, Apart from the change in intensitites and a few peak shifts, no new peaks emerged in the modified samples. As shown in the figure 29 below the modified materials also showed the relative intensities for the substrate material which in case of SuFe was identified to be hydronium jarosite with following dominant peak intensities [0 2 1], [1 1 3] and [0 1 2]. For CaFe the phase was identified to be bassanite with the following donimant peaks [1 1 -1], [2 2 -2] and [5 1 -1].

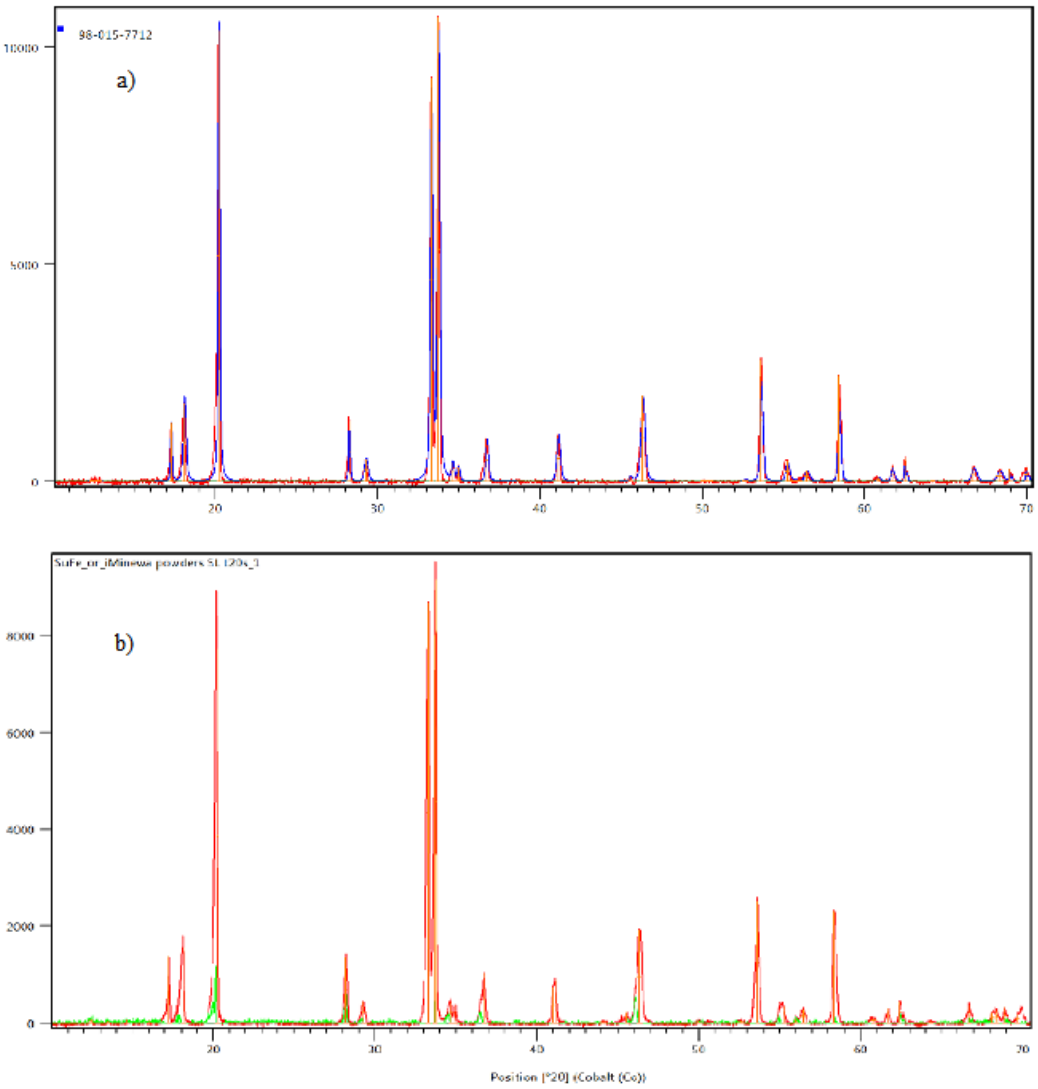

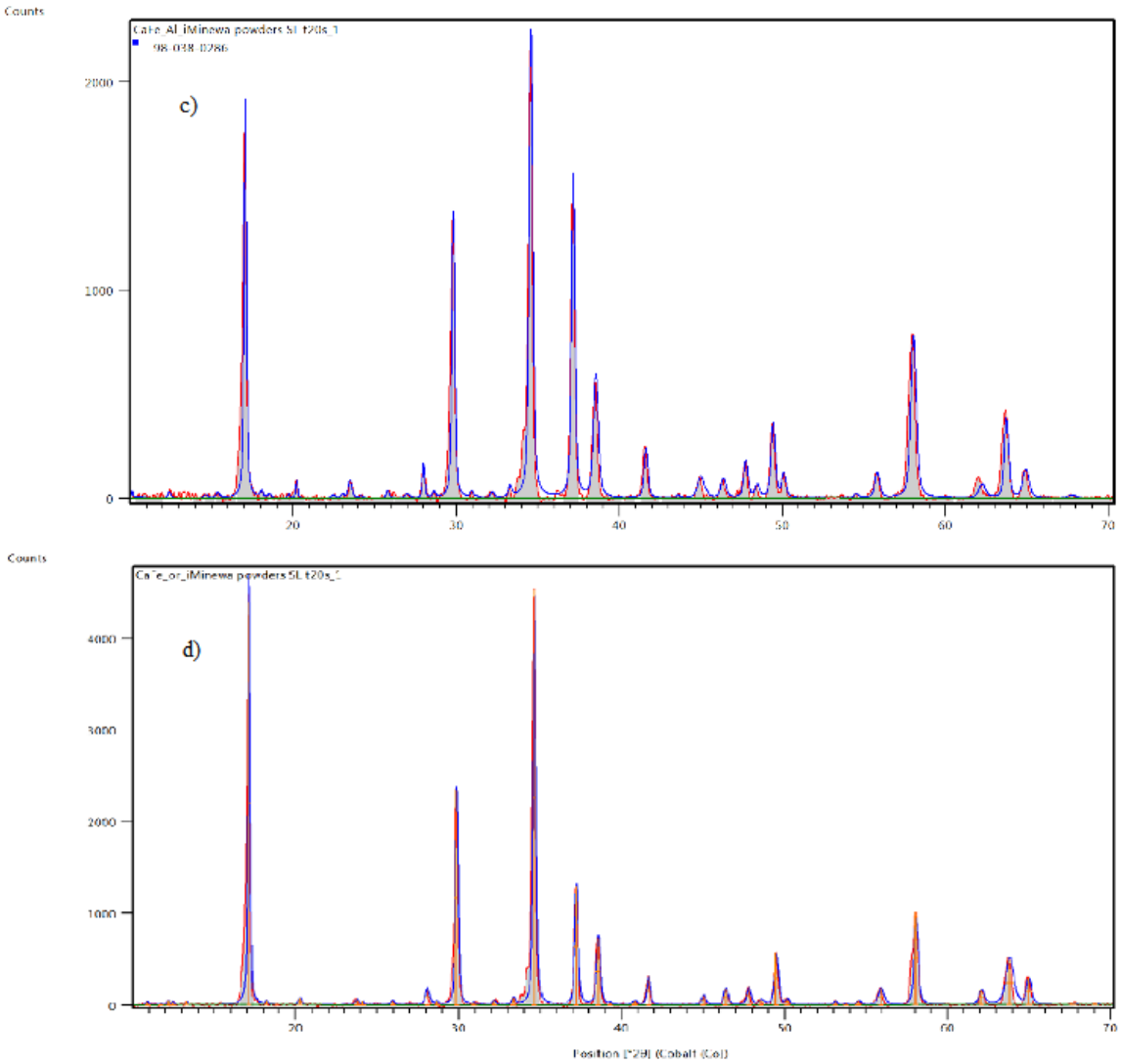

Figure 32. XRD patterns a) SuFe_Al_2O_3, b) SuFe Original, c) CaFe_Al_2O_3, d) CaFe Original.

The nature of the interstitial porous system of the adsorbents can be studied from the BET Please, remove or give number of this paragraph isotherms. The figure 30 illustrates N_2 adsorption-desorption isotherm curves obtained at 77 K plotted as a function of relative pressure which is the equilibrium pressure divided by saturation pressure (P/P_o). As per IUPAC classification, all the unmodified and modified adsorbents (RH, SuFe, CaFe) shows type III isotherm with H3 hysteresis reversible loops in the range of 0.5 to 0.8. Due to the absence of the flat plateau in the curve, it can be concluded that there is no monolayer formation but multilayer. Additionally, type III curve is also characteristic of non-porous solids.

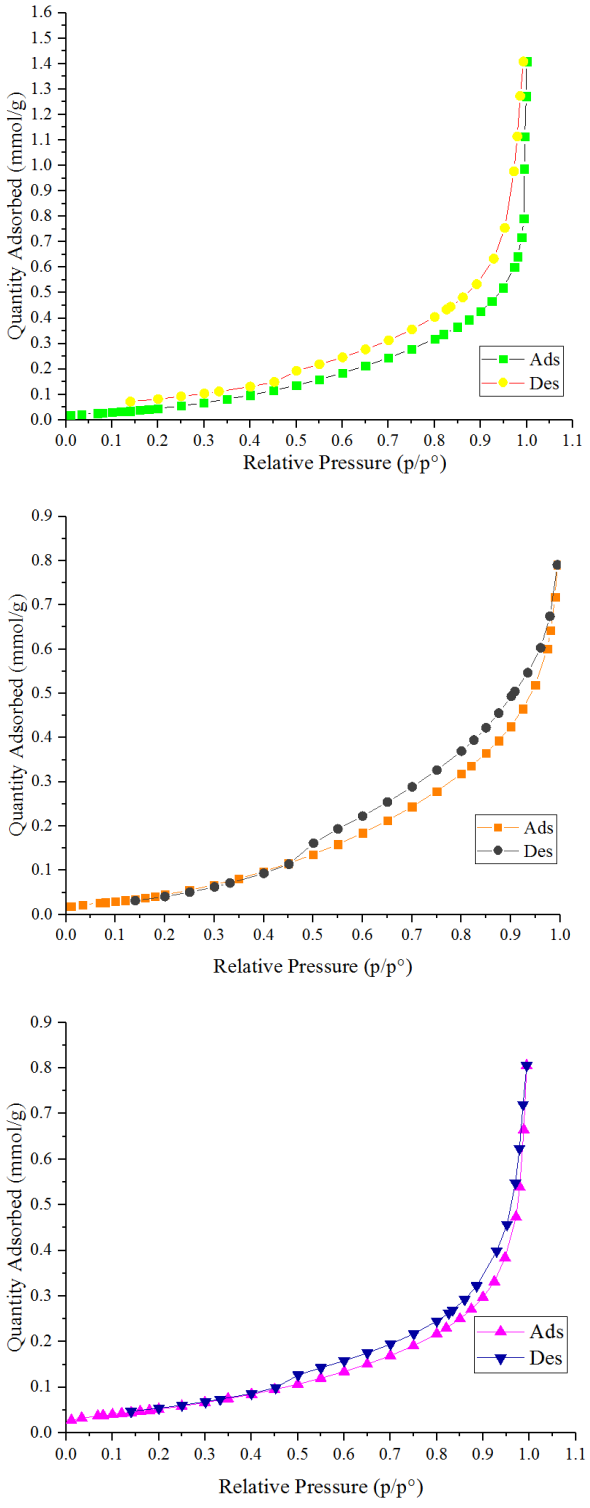

Figure 33. BET isotherm cuves for a) RH_Original, b) RH_Al_2O_3 c) RH_TiO_2.

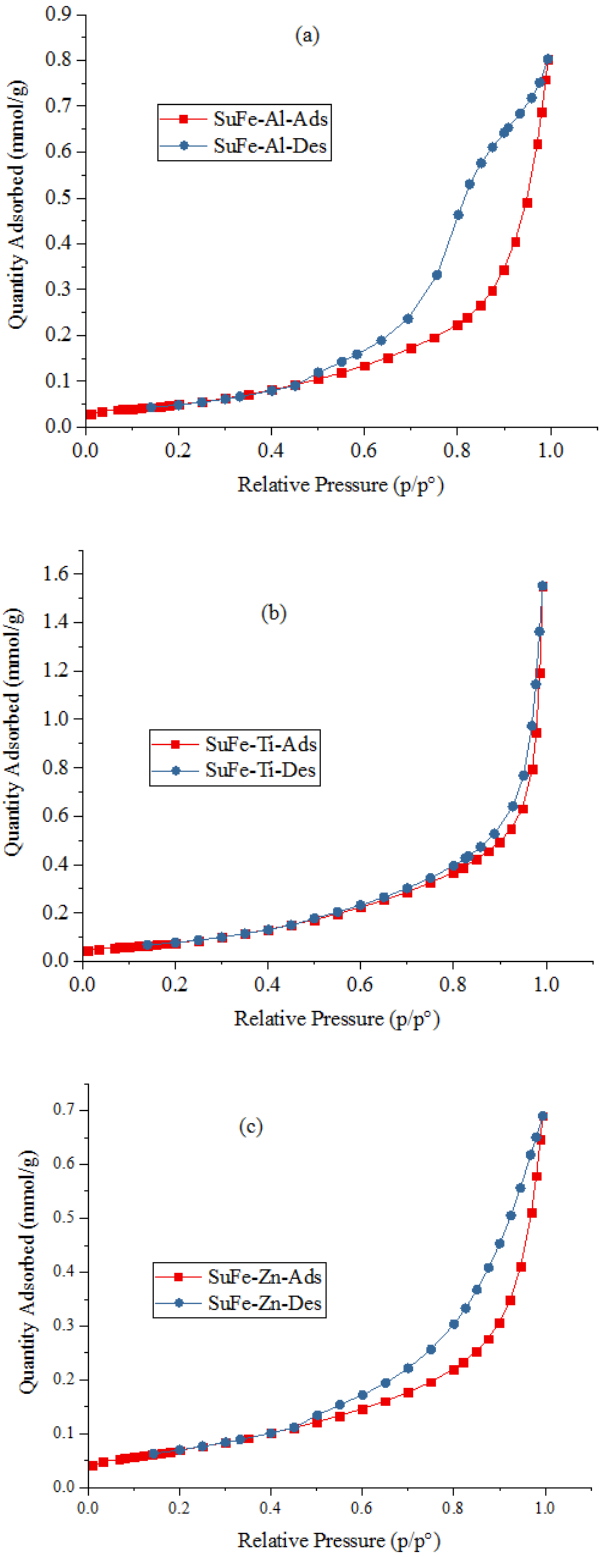

Figure 34. BET isotherm curves for a) SuFe-Al, b) SuFe-Ti, c) SuFe-Zn.

The desorption shoulders and closure points observed in 0.5 P/P_0 region of N_2 adsorption at 77K are also conspicuous in the plots as well, with the H2, H3 and H4 loops all being similar. An important observation to be pointed includes the absence of plateau at high pressure ratio regions. This is due to the non-existence of a distinct mesopore volume in such regions and hence such plots should not be misinterpreted as Type IV isotherm and treated with caution (Rouquerol *et al.* 1999). A close resemblance to the type II isotherm is observed despite the presence of an initial reversible monolayer-multilayer zone (Sing *et al.* 1985). Such a deviation from the true behavior of type II isotherm can be highlighted via the construction of comparison plot (Rouquerol *et al*. 1999). There may be a number of factors attributing to such a pseudo behavior of the isotherm. Metastability of the adsorbed multilayer and delayed capillary action with non-rigidity of the aggregate structure and low pore curvature being the predominant ones. Also the non-rigid structure of the adsorbent affects the observed hysteresis loop.

It is very important to determine the isoelectric pH of the adsorbent as it indicates the pH at which the net charge is zero. The charge is created on the surface of the adsorbents owing to the protonation and deprotonation of the surface functional groups, forming an electric double layer. Therefore, knowing the zeta potential values over the range of pH yields a possibility to understand the mechanism behind the adsorption between the target ions and the adsorbents. In this study, the zeta potential measurements were carried out over the pH regime of 1-10, the results of which are shown in figure 32.

The Zeta potential curves were plotted as a function of the pH values for all the adsorbents. In the case of RH samples, there is a decreasing trend in the zeta potential observed with an increase in the pH values. However, the slope of the trend line is not similar in both modified and unmodified samples. The decrease in zeta potential observed in the unmodified adsorbent is not much as compared to the other two adsorbents. The RH_Al_2O_3 samples show a sudden drop in the potential values followed by a moderate slope for the plot, while the RH_TiO_2 samples demonstrate a sharp decrease throughout the pH range with almost a constant slope. The maximum negative zeta potential values of the unmodifed case is almost half that of the modified cases around pH 8.

For the next set of samples under study involving SuFe unmodified and modified cases (TiO_2 and Al_2O_3 modifications), the unmodified case depicts a gradual decrease in the zeta potential values in the pH range under consideration. The SuFe-TiO_2 samples display a very small reduction in the potential values from pH 2 till 4 and beyond which the values remain almost similar. On the other hand, though there is not much change in zeta potential values for SuFe-Al_2O_3 modified samples until pH 7, there is drastic redcution seen above pH 7.

Unlike the other samples under study, for which the initial zeta potential values in lower pH regime are positive, the CaFe samples have negative zeta potential even from pH 2. A similar trend in the potential curves are observed for all the cases i.e. modified and unmodified, where there is a gradual decrease in the values until pH 7 followed by an acute reduction. The lowest potential values are shouldered by the unmodified CaFe samples. From an overall perspective, the plots depict that after modification with Al_2O_3 and TiO_2, the zeta potential seem to shift towards positive potential. However, they don't exhibit higher positive potential as seen in SuFe samples at the lower pH regime. It might be due to the fact that Fe content is higher in SuFe than CaFe which makes SuFe susceptible to higher positive potential.

For cyanide removal study, SuFe-Al_2O_3 and CaFe-Al_2O_3 adsorbents were selected because Ferrocyanide complex is expected to form as a result of reaction between Fe^{2+} and CN^- ions. Hence the adsorbents should possess positive charge on the surface in order to adsorb negatively charged Cyanide ions, which is the same case of SuFe-Al_2O_3 and CaFe- Al_2O_3. The electrostatic attraction between the positively charged adsorbents and the negatively charged cyanide ions is expected to be the main reason behind the interaction between the Cyanide ions and the adsorbents.

On the other hand, for the removal of cations such as Fe^{2+}, Cu^{2+}, Zn^{2+} and Ni^{2+}, RH modified adsorbents would be ideal as they documented negative potential values of below - 10 from pH 4. This would result in the electrostatic attraction between the positively charged cations and negatively charged RH adsorbents. Due to this affinity, the higher adsorption of the target cations is expected to occur predominantly in this pH range.

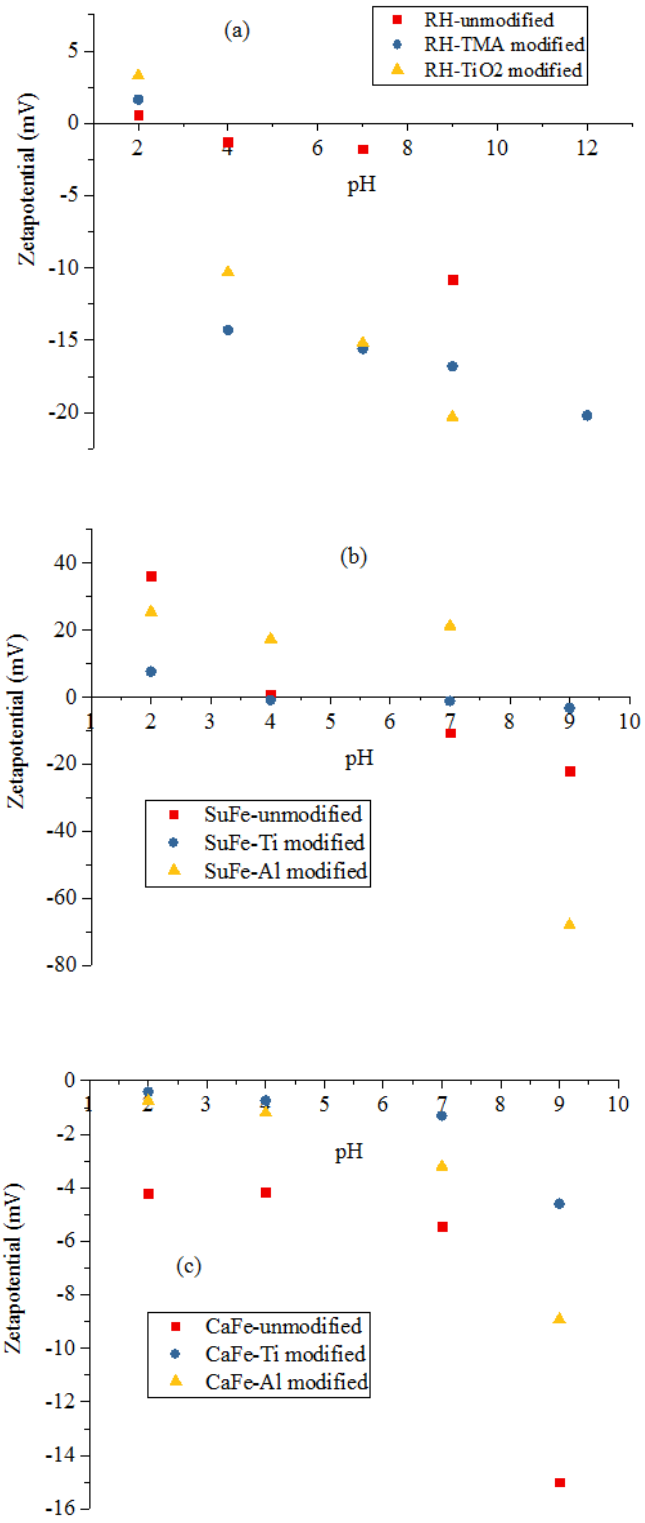

Figure 35. Zetapotential curves for a) RH, b) SuFe, c) CaFe, before and after modification.

4.2. AMD treatment

The optimum amount of adsorbent was found mixing different concentrations 1, 2, 5, 10, 20, 30, 40 and 50 gL^{-1} of adsorbents into 45mL of synthetic AMD. Separate solution with known concentration of metallic ions were used for this, mixing the original RH, TiO_2 modified and finally Al_2O_3 modified RH. The effect of dosage amount was quite impressive as the modified materials actively removed the targeted metallic ions with concentrations nearly 20 times less than that of original RH material. Figure 33 shows the removal of SO_4^{2-} as a function of concentration of adsorbents, the best these could manage is nearly 70-80% removal, but the concentration of modified adsorbents needed for that is quite low, nearly 2-3 gL^{-1}.

The removal for metal ions (figure 34, 35) seemed quite better, around 99% removal was achieved within 2-3 gL^{-1} concentration of the adsorbents.

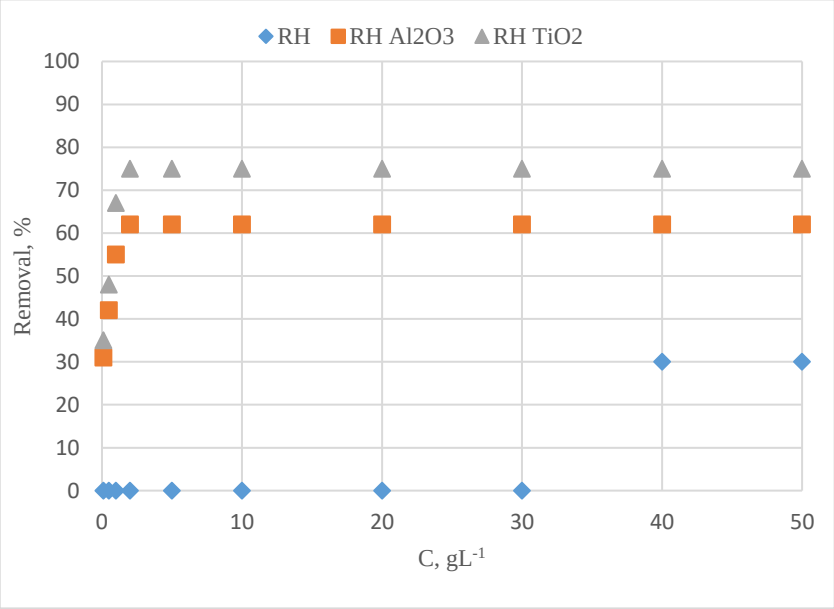

Figure 36. Removal of SO_4^{2-}, effect of amount of RH, RH_TiO_2 and RH_Al_2O_3 (Iakovleva et al., under review).

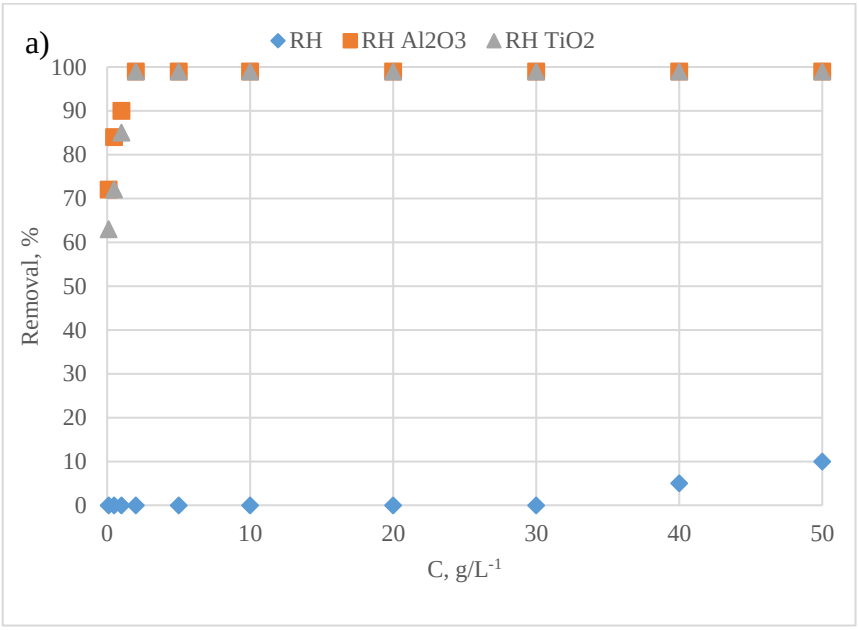

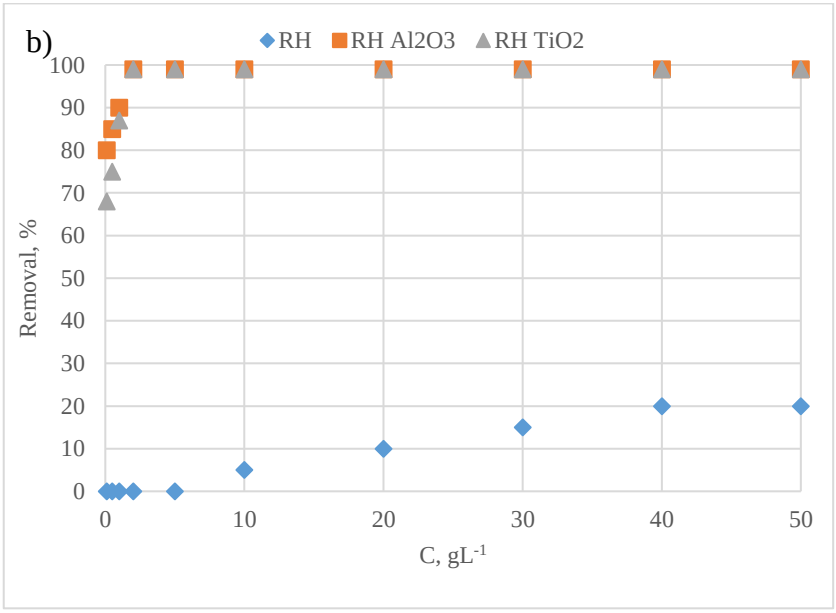

Figure 37. Removal of a) Ni^{2+} and b) Zn^{2+}, effect of amount of RH, RH_TiO_2 and RH_Al_2O_3 (Iakovleva et al., under review).

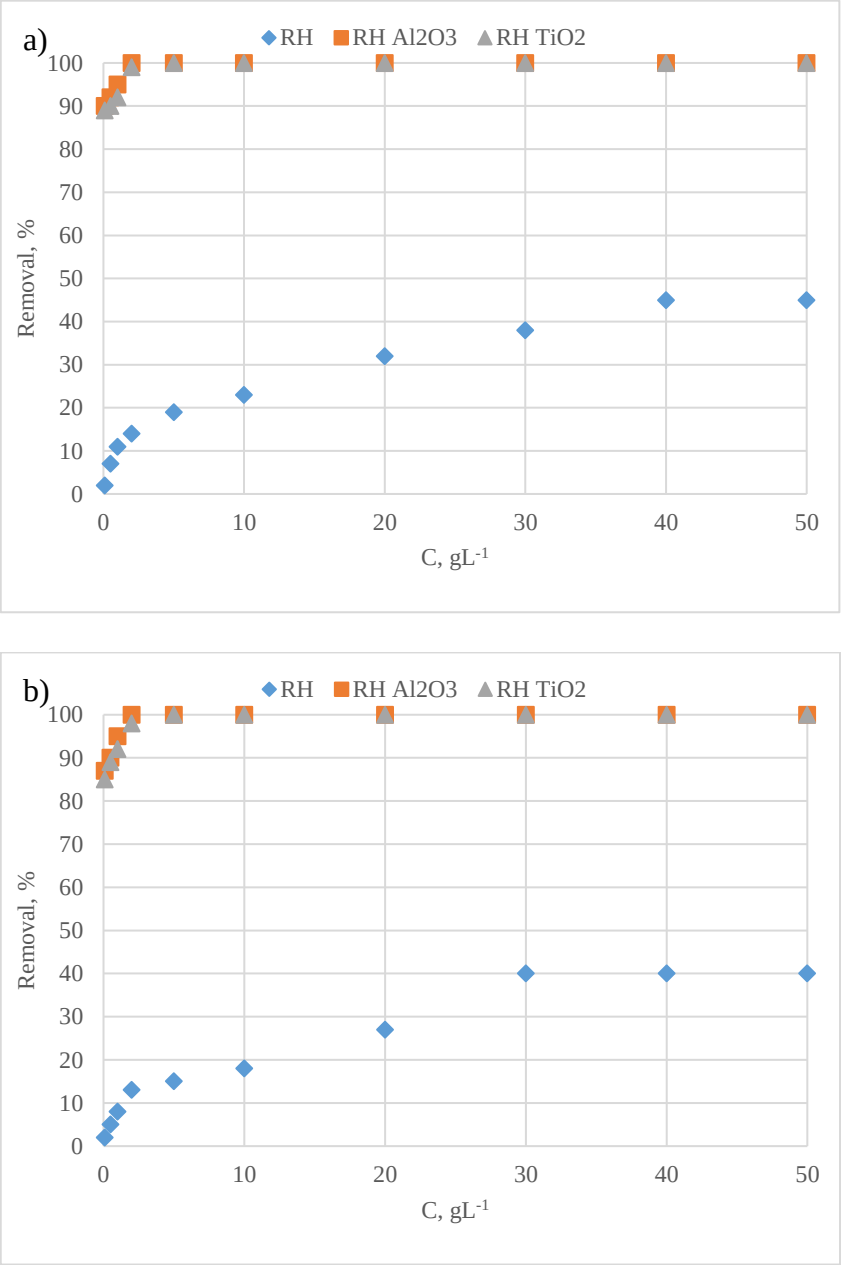

Figure 38. Removal of a) Fe^{3+} and b) Cu^{2+}, effect of amount of RH, RH_TiO_2 and RH_Al_2O_3 (Iakovleva et al., under review).

4.2.1. Equilibrium modeling

The interaction between the adsorbents and adsorbates is defined by one of isotherm models defined earlier, for this case Langmuir adsorption isotherm was employed to understand the interaction. The general equation used for this model is as follows:

$$q_e = \frac{q_m k_L C_e}{1 + k_L C_e} \tag{18}$$

Where in this equation q_e (mmol/g) is equilibrium sorption capacity and q_m mmol/g is the maximum adsorption capacity. Where K_L is Langmuir constant and C_e (mmol/L) is the concentration of contaminant ions in the solution.

The values of R^2 of linear plot (table 13) of Langmuir isotherm were found quite satisfactory at temperature 25°C, where the equation works in a way that assuming an energetically homogeneous surface of adsorbent and only the monolayer coverage (Bhatt et al., 2012). To approximate the error with the difference between the experimental and calculated valued ions adosrbed, following equation was used:

$$\Sigma_i^n = \left(\frac{(q_{e,\exp} - q_{e,calc})^2}{q_{e,exp}} \right)_i \tag{19}$$

Where $q_{e,exp}$ and $q_{e,calc}$ being the experimental and calculated values respectively.

The parameter q_m in equation 10 depicts the number of adsorbent sites which may interact with the contaminants. Looking at the table 13, it is quite evident that this value increases many fold with the modified adsorbents as compared to original RH, especially for sulfates it goes above 600mmol g^{-1}. Same goes for the adsorbent - adsorbate interaction parameter K_L here it is the lowest for Ni ions, showing the least affinity of the adsorbents towards Ni as compared to other ions. The trend found can be stacked in order as follows:

$Fe^{3+} > Cu^{2+} > SO_4^{2-} > Zn^{2+} > Ni^{2+}$

Table 12. Adsorption isotherms parameters for original and modified RH adsorbent (Iakovleva et al., under review).

Adsorbents	Ions	C_e (mmol L^{-1}	$q_{e\ exp}$ (mmol g^{-1})	$q_{e\ model}$ (mmol g^{-1})	q_m (mmol g^{-1})	K_L (L $mmol^{-1}$)	R^2
RH	SO_4^{2-}	47.4	11.72	11.24	11.37	18.68	0.73
	Ni^{2+}	1.69	0.11	0.10	0.12	9.01	0.70
	Zn^{2+}	1.54	0.20	0.19	0.17	12.03	0.75
	Cu^{2+}	1.56	0.39	0.40	0.38	21.09	0.82
	Fe^{3+}	1.78	0.75	0.72	0.74	25.12	0.87
RH_Al_2O_3	SO_4^{2-}	47.4	650	622	637	20.15	0.82
	Ni^{2+}	1.69	98	100	99	10.17	0.85
	Zn^{2+}	1.54	150	145	152	12.05	0.84
	Cu^{2+}	1.56	201	204	199	20.22	0.87
	Fe^{3+}	1.78	225	215	218	26.30	0.90
RH_TiO_2	SO_4^{2-}	47.4	623	620	625	21.30	0.95
	Ni^{2+}	1.69	85	83	87	9.6	0.85
	Zn^{2+}	1.54	137	136	138	12.5	0.85
	Cu^{2+}	1.56	190	185	187	20.3	0.90
	Fe^{3+}	1.78	215	210	217	25.7	0.93

4.3. Removal of Cyanides

A 15mL of cyanide ion solution was used mixed with varying amounts of adsorbents (1, 2, 5, 10, 20, 30, 40, 50 g/L). As the figure 36 shows below the optimum amount before equilibrium for both unmodified adsorbents is 10g/L as opposed to 5g/L concentration of modified sorbents. However, both modified and unmodified adsorbents successfully reached cyanide removal percentage of 97%.

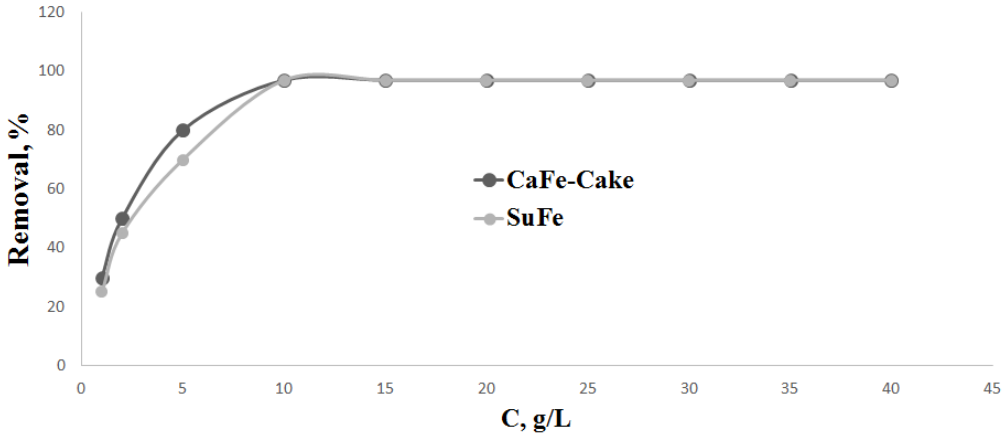

Figure 39. Effect of adsorbent dosage on cyanide removal for original SuFe and CaFe materials (Iakovleva et al., under review).

To notice the effect of contact time of adsorbents on the removal of cyanide ions, a 20 mg/L of cyanide solution was mixed with 40g/L of original solutions. The time was varied from 30-720 mins as 30, 60, 120, 240, 360 and finally 720 mins. For original materials the equilibrium reached at 360 mins while for modified samples it took 210 mins for the maximum percentage removal.

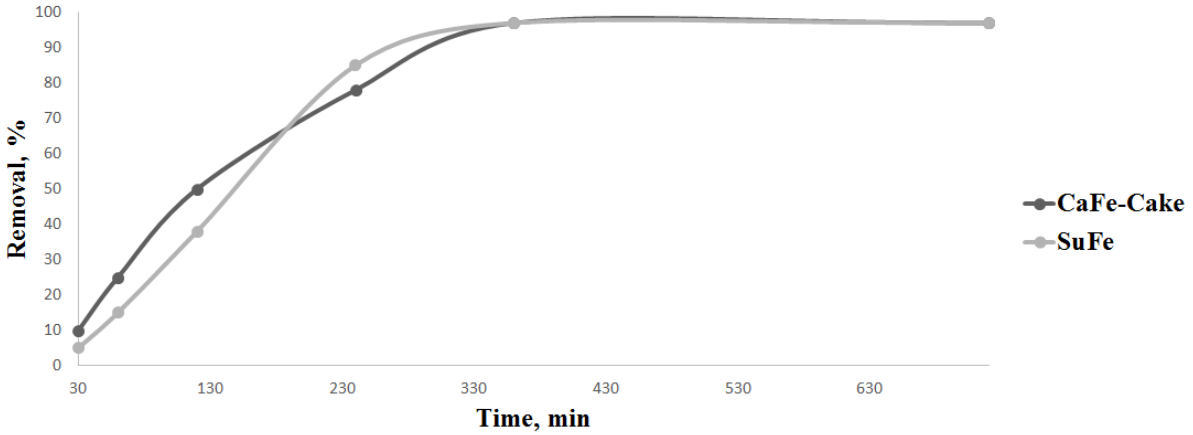

Figure 40. Effect of contact time on cyanide removal for orignal SuFe and CaFe (Iakovleva et al., under review).

Selection of pH for the batch adsorption experiments is very necessary, therefore a study was performed to notice the effect of pH on the removal of cyanide ions. As shown in figure 38 below the removal is quite consistent with pH till 4 showing 97% removal, crossing that it drops down quite fast specially for CaFe material around 70% and SuFe around 80%. This further deteriorates as we move towards higher pH values, thus pH 4 was selected as optimum.

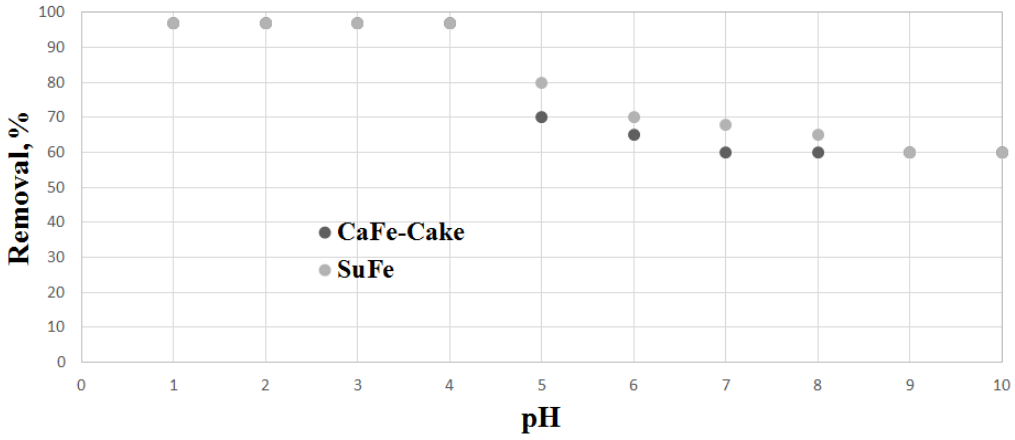

Figure 41. Effect of pH on removal of cyanide ions (Iakovleva et al., under review).

4.3.1. Equilibrium modeling

For the removal of cyanides, the interaction between adsorbent and adsorbate is approximated with two isotherms, Langmuir and Freundlich models, equation 12 and 13 respectively. The difference between the experimental and calculated values of ions adsorbed depicted by Freundlich model were quite less, whereas the difference was slightly more in case of Langmuir model. Many heterogeneous surfaces can be explained with Freundluch model since it assumes multisite adsorption for heterogeneous surfaces given the heterogeneity factor (Bhatt et al., 2012) defined as 'n' as shown in equation below, and showing almost near unity r^2 values.

Langmuir on the other hand assumes rather energetically homogeneous surface of adsorbent, explains a bit lower r^2 values. The error is calculated by equation 14 known as Marquardt's percent standard deviation.

$$q_e = \frac{q_m k_L C_e}{1 + k_L C_e} \tag{20}$$

$$\ln(Q_e) = \ln(K_F) + \frac{1}{n_F}\ln(C_e) \tag{21}$$

$$\Sigma_i^n = \left(\frac{(q_{e,\exp} - q_{e,calc})^2}{q_{e,exp}}\right)_i \tag{22}$$

The value of heterogeneity factor 'n' being less than 1 indicates the adsorption behavior to be chemical process, forming complex cyanide ions thus removing cyanide from water, but the adsorbents are limited to one time use only.

Table 13. Langmuir and Freundlich isotherm parameters for modified and unmodified CaFe and SuFe(Iakovleva et al., under review).

	$q_{m\ exp}$, mmol/g	K L/mmol	n	R^2
Langmuir model				
CaFe-Cake	3.10	3.87		0.75
CaFe-Cake_Al_2O_3	15.2	3.95		0.82
SuFe	3.31	2.68		0.78
SuFe_Al_2O_3	15.0	2.72		0.80
Freundlich model				
CaFe-Cake	3.52	5.45	0.62	0.99
CaFe-Cake_Al_2O_3	15.5	6.01	0.62	0.99
SuFe	3.72	6.18	0.57	0.98
SuFe_Al_2O_3	15.8	6.22	0.60	0.98

Real AMD was tested with modified and unmodified RH samples; same batch method was used with 2g/L of RH-TiO2 and RH-Al2O3. The percentage removal for SO_4^{2-}, Ni^{2+}, Zn^{2+}, Fe^{3+} and Cu^{2+} was tested, which however was quite lower as compared to synthetic AMD. The percentage removed was 50%, 75%, 80%, 99% and 90 for SO_4^{2-}, Ni^{2+}, Zn^{2+}, Fe^{3+} and Cu^{2+} respectively. In real AMD there are other ions in competition apart from the targeted ions, which might have slightly more affinity towards adsorbents.

CONCLUSION

In this research an attempt was made to employ the industrial solid waste and some sulfate tailings as potential adsorbents for mine water treatment. The results presented in this study show that these waste materials with modifications done by atomic layer deposition show good enough adsorbent properties to remove contaminant ions from mine water. Using atomic layer deposition for powder materials is an emerging field with challenges, however, optimal conditions and recipes were prepared to develop these metallic oxides on the substrates.

A comparison was made to show the improved tendencies in the modified materials, a number of characterization methods were used to see the changes made in structure and morphology of the adsorbents, a number of which point in better adsorbent properties of these materials. An attempt was also made to treat real AMD with RH modified materials, which showed quite promising result showing ion removal in following order:

$Fe^{3+} > Cu^{2+} > Zn^{2+} > Ni^{2+} > SO_4^{2-}$

Sulfate tailings on the other hand could manage to attain removal efficiency of around 97%, selectively removing cyanide ions from synthetic mine water. Both the concentration and adsorption time was reduced in modified samples but one drawback was only one time use of the adsorbents. Future studies can be carried out to improve regeneration properties of these adsorbents. Since coating the adsorbents with metallic oxides have tend to increase their properties, if some cheaper and equally as efficient process as ALD is used these adsorbents can be prepared being economically viable, for now the process being quite expensive. Some other industrial waste materials hard to dispose can find their potential use with or without modifications carrying forward the theme of this study towards green future.

REFERENCES

1. Akcil, A. and Koldas, S. (2006). Acid Mine Drainage (AMD): causes, treatment and case studies. Journal of Cleaner Production, 14(12-13), pp.1139-1145.
2. Azizullah, A., Khattak, M., Richter, P. and Häder, D. (2011). Water pollution in Pakistan and its impact on public health — A review. *Environment International*, [online] 37(2), pp.479-497. Available at: http://www.sciencedirect.com/science/article/pii/S0160412010002060.
3. Bagherani, N. and R Smoller, B. (2016). An overview of zinc and its importance in dermatology- Part I: Importance and function of zinc in human beings. *Global Dermatology*, 3(5), pp.330-336.
4. Barakat, M. (2011). New trends in removing heavy metals from industrial wastewater. *Arabian Journal of Chemistry*, 4(4), pp.361-377.
5. Barrer, R.M. (1989) Pure Appl. Chem. 61, 1903.
6. Bhatnagar, A., Hogland, W., Marques, M. and Sillanpää, M. (2013). An overview of the modification methods of activated carbon for its water treatment applications. Chemical Engineering Journal, 219, pp.499-511.
7. Bhatnagar, A. and Sillanpää, M. (2010). Utilization of agro-industrial and municipal waste materials as potential adsorbents for water treatment—A review. *Chemical Engineering Journal*, 157(2-3), pp.277-296.
8. Bhatt, A., Sakaria, P., Vasudevan, M., Pawar, R., Sudheesh, N., Bajaj, H. and Mody, H. (2012). Adsorption of an anionic dye from aqueous medium by organoclays: equilibrium modeling, kinetic and thermodynamic exploration. *RSC Advances*, [online] 2(23), p.8663. Available at: https://www.researchgate.net/publication/236165917_Adsorption_of_an_Anionic_Dye_from_Aqueous_Medium_by_Organoclays_Equilibrium_Modeling_Kinetic_and_Thermodynamic_Exploration.
9. Cui, J., Du, Y., Xiao, H., Yi, Q. and Du, D. (2014). A new process of continuous three-stage co-precipitation of arsenic with ferrous iron and lime. Hydrometallurgy, 146, pp.169-174.

10. Dąbrowski, A., Hubicki, Z., Podkościelny, P. and Robens, E. (2004). Selective removal of the heavy metal ions from waters and industrial wastewaters by ion-exchange method. Chemosphere, 56(2), pp.91-106.
11. Directive 2006/21/EC of the European parliament and of the council of 15 March 2006 on the management of waste from extractive industries and amending Directive 2004/35/EC (OJ L 102, 11.4.2006, p. 15)
12. Ec.europa.eu. (2016). *Waste statistics - Statistics Explained*. [online] Available at: http://ec.europa.eu/eurostat/statistics-explained/index.php/Waste_statistics [Accessed 5 Feb. 2017].
13. Eisler, R. and S.N. Wiemeyer. Cyanide Hazards to Plants and Animals from Gold Mining and Related Water Issues. Reviews of Environmental Contamination and Toxicology, 2004. 183: p. 21-54.
14. Ferrante, M., Conti, G., Rasic-Milutinovic, Z. and Jovanovic, D. (2013). *Health effects of metals and related substances in drinking water*. IWA Publishing: International Water Association.
15. Fortin, J., Desmettre, T., Manzon, C., Judic-Peureux, V., Peugeot-Mortier, C., Giocanti, J., Hachelaf, M., Grangeon, M., Hostalek, U., Crouzet, J. and Capellier, G. (2010). Cyanide Poisoning and Cardiac Disorders: 161 Cases. *The Journal of Emergency Medicine*, 38(4), pp.467-476.
16. Fu, F. and Wang, Q. (2011). Removal of heavy metal ions from wastewaters: A review. Journal of Environmental Management, 92(3), pp.407-418.
17. Gaikwad, R., Sapkal, R. and Sapkal, V. (2010). Removal of Copper Ions from Acid Mine Drainage Wastewater Using Ion Exchange Technique: Factorial Design Analysis. JWARP, 02(11), pp.984-989.
18. Geological survey of Finland. (2016). *List of mining projects in Finland*. [online] Available at: http://en.gtk.fi/export/sites/en/informationservices/maps/GTK_kaivokset_ja_tutkimuskohteet.pdf [Accessed 22 Sep. 2016].
19. Gupta, V. and Suhas, (2009). Application of low-cost adsorbents for dye removal – A review. *Journal of Environmental Management*, 90(8), pp.2313-2342.

20. Hegazi, H. (2013). Removal of heavy metals from wastewater using agricultural and industrial wastes as adsorbents. *HBRC Journal*, 9(3), pp.276-282.
21. Iakovleva, E., Mäkilä, E., Salonen, J., Sitarz, M., Wang, S. and Sillanpää, M. (2015). Acid mine drainage (AMD) treatment: Neutralization and toxic elements removal with unmodified and modified limestone. Ecological Engineering, 81, pp.30-40.
22. Iakovleva, E., Maydannik, P., Ivanova, T., Sillanpää, M., Tang, W., Mäkilä, E., Salonen, J., Gubal, A., Ganeev, A., Kamwilaisak, K. and Wang, S. (2016). Modified and unmodified low-cost iron-containing solid wastes as adsorbents for efficient removal of As(III) and As(V) from mine water. *Journal of Cleaner Production*, 133, pp.1095-1104.
23. Iakovleva, E., Sillanpää, M., Mangwandi, C., Albadarin, A., Allen, S., Maydannik, P., Khan, S., Mäkilä, E., Salonen, J., Kamwilaisak, K. and Wang, S. (under review). Atomic layer deposition of Al_2O_3 onto the granulated sulphate tailings for efficient removal of cyanide from mine wastewater.
24. Iakovleva, E., Sillanpää, M., Maydannik, P., Khan, S., Kamwilaisak, K. and Wang, S. (under review). Novel sorbents from low-cost materials modified with atomic layer deposition for acid mine drainage treatment.
25. Jacobs, J., Lehr, J. and Testa, S. (2014). Acid mine drainage, rock drainage, and acid sulfate soils.
26. Jaria, G., Silva, C., Ferreira, C., Otero, M. and Calisto, V. (2017). Sludge from paper mill effluent treatment as raw material to produce carbon adsorbents: An alternative waste management strategy. *Journal of Environmental Management*, 188, pp.203-211.
27. Kilislioglu, A. ed., (2015). Ion Exchange - Studies and Applications. 1st ed. InTech.
28. Kilislioglu, A. ed., (2015). Ion Exchange - Studies and Applications. 1st ed. InTech.
29. Lenntech.com. (2016). *Iron removal by physical chemical way*. [online] Available at: http://www.lenntech.com/processes/iron-manganese/iron/iron-removal-physical-chemical-way.htm [Accessed 10 Nov. 2016].
30. Lottermoser, B. (2007). Mine wastes. Berlin: Springer.
31. Mastai, Y. (2013). *Materials Science - Advanced Topics*. InTech, p.Chapter 3. Atomic Layer Deposition on Self-Assembled- Monolayers.

32. Masukume, M., Onyango, M. and Maree, J. (2014). Sea shell derived adsorbent and its potential for treating acid mine drainage. *International Journal of Mineral Processing*, 133, pp.52-59.
33. McKay, G. (1996). *Use of adsorbents for the removal of pollutants from wastewaters*. 1st ed. Boca Raton: CRC Press.
34. McPherson, R., Pincus, M. and Henry, J. (2007). *Henry's clinical diagnosis and management by laboratory methods*. Philadelphia: Saunders Elsevier.
35. Mortazavi, S. (2008). *Application of membrane separation technology to mitigation of mine effluent and acidic drainage*. [online] Mining Association of Canada, pp.5, 38-50. Available at: http://mend-nedem.org/wp-content/uploads/2013/01/3.15.1.pdf [Accessed 27 Sep. 2016].
36. Pall Corporation. (2016). Mine Water Treatment: Filtration and Separation Technologies for Mine Water Treatment. [online] Available at: https://www.pall.com/pdfs/Industrial-Manufacturing/MEMWTEN_Pall_Mine_Water_Treatment.pdf [Accessed 23 Sep. 2016].
37. Perk, M. (2013). *Soil and Water Contamination, 2nd Edition*. Hoboken: CRC Press.
38. Pivnyak, G., Bondarenko, V., Kovalevs'ka, I. and Illiashov, M. (2013). Mining of mineral deposits. Leiden, The Netherlands: CRC Press/Balkema.
39. Qu, H. and Liu, S. (2014). Removal of Heavy Metal Ions from Waste Water Using Modified Sands: A Brief Review. *KEM*, 636, pp.65-68.
40. Qureshi, A., Maurice, C. and Öhlander, B. (2016). Potential of coal mine waste rock for generating acid mine drainage. *Journal of Geochemical Exploration*, [online] 160, pp.44-54. Available at: http://www.sciencedirect.com.ludwig.lub.lu.se/science/article/pii/S0375674215300881?np=y&npKey=9eb46e1ba8ae0556bfabbdfccb046c82180827f55a2dfcadb0d54e14082ad7a2.
41. Rgs.org. (2017). Royal Geographical Society (with IBG): the heart of geography. [online] Available at: http://www.rgs.org/HomePage.htm [Accessed 04 Jan. 2017].
42. Rouquerol, F., Rouquerol, J. and Sing, K. (1999) Adsorption by Powders and Porous Solids, Academic Press, London.

43. Saria, L. (2006). Leaching of heavy metals in acid mine drainage. *Waste Management & Research*, 24(2), pp.134-140.
44. Separationprocesses.com. (2016). *Introduction to Membrane*. [online] Available at: http://www.separationprocesses.com/Membrane/MT_Chp01.htm [Accessed 27 Sep. 2016].
45. Sharma, S. (2014). *Heavy Metals In Water: Presence, Removal and Safety*. Royal Society of Chemistry.
46. Sheoran, A. and Sheoran, V. (2006). Heavy metal removal mechanism of acid mine drainage in wetlands: A critical review. Minerals Engineering, 19(2), pp.105-116.
47. Siddharth, S., Jamal, A., Dhar, B. and Shukla, R. (2002). Acid-Base Accounting: A Geochemical Tool for Management of Acid Drainage in Coal Mines. *Mine Water and the Environment*, 21(3), pp.106-110.
48. Sillanpää, M. (2015). *Natural organic matter in water; Characterization and Treatment Methods*. 1st ed. Elsevier Inc., pp.213-238.
49. Simate, G. and Ndlovu, S. (2014). Acid mine drainage: Challenges and opportunities. *Journal of Environmental Chemical Engineering*, 2(3), pp.1785-1803.
50. Simate, G., Maledi, N., Ochieng, A., Ndlovu, S., Zhang, J. and Walubita, L. (2016). Coal-based adsorbents for water and wastewater treatment. *Journal of Environmental Chemical Engineering*, 4(2), pp.2291-2312.
51. Sing, K.S.W., Everett, D.H., Haul, R.A.W., Moscou, L., Pierotti, R.A., Rouquerol, J. and Siemieniewska, T. (1985) Pure Appl. Chem. 57, 603.
52. Singh, G. (1986). A survey of corrosivity of underground mine waters from indian coal mines. *International Journal of Mine Water*, [online] 5(1), pp.21-32. Available at: https://www.imwa.info/bibliographie/05_1_021-032.pdf.
53. Solar, C., García, A., Vallone, A. and Sapag, K. (2016). Adsorption of methane in porous materials as the basis for the storage of natural gas. [online] pp.215-216. Available at: http://cdn.intechopen.com/pdfs/11484/InTech-Adsorption_of_methane_in_porous_materials_as_the_basis_for_the_storage_of_natural_gas.pdf [Accessed 10 Nov. 2016].
54. Stewart, W., Miller, S. and Smart, R. (2006). aAdvances in acid rock drainage (ard) characterisation of mine wastes. *JASMRR*, 2006(2), pp.2098-2119.

55. Strohfeldt-Venables, K. (2015). *Essentials of Inorganic Chemistry: For Students of Pharmacy, Pharmaceutical*. John Wiley & Sons.
56. Sundew Technologies, Llp, (2017). *Capacitors with high energy storage density and low esr*. WO2006014753 A1.
57. Suntola, T. and Simpson, M. (1990). *Atomic layer epitaxy*. 1st ed. Glasgow: Blackie.
58. Tuutijärvi, T., Lu, J., Sillanpää, M. and Chen, G. (2009). As(V) adsorption on maghemite nanoparticles. *Journal of Hazardous Materials*, 166(2-3), pp.1415-1420.
59. Ultratech/CNT. (2017). *Ultratech/CNT: Leading ALD Research*. [online] Available at: http://cambridgenanotechald.com/atomic-layer-deposition.shtml [Accessed 10 Nov. 2016].
60. UNEP/OCHA. The Cyanide Spill at Baia Mare, Romania: Before, During and After. P. Csagoly, Editor. 2000. The Regional Environmental Center for Central and Eastern Europe. Available: http://archive.rec.org/REC/Publications/CyanideSpill/ENGCyanide.pdf
61. Vhahangwele, M. and Mugera, G. (2015). The potential of ball-milled South African bentonite clay for attenuation of heavy metals from acidic wastewaters: Simultaneous sorption of Co2+, Cu2+, Ni2+, Pb2+, and Zn2+ ions. *Journal of Environmental Chemical Engineering*, 3(4), pp.2416-2425.
62. W. Thomas and B. Crittenden, Adsorption technology and design. Oxford: Butterworth-Heinemann, 1998.
63. Wang, L., Hung, Y. and Shammas, N. (2005). *Physicochemical treatment processes*. Totowa, N.J.: Humana Press.
64. Warren, L.A. (2011). Acid Rock Drainage. Encyclopedia of Geobiology, pp. 5-8. Netherlands: Springer.
65. Wolkersdorfer, C. (2008). *Water management at abandoned flooded underground mines*. Berlin: Springer, pp.9-30.
66. Worch, E. (2012). *Adsorption technology in water treatment*. 1st ed. Berlin: De Gruyter.
67. World Health Organization, Guidelines for drinking-water quality, 2nd ed. Vol. 2. Health criteria and other supporting information. World Health Organization, Geneva, 1996.

68. World-Mining-Data, C. Reichl, M. Schatz, G. Zsak, Volume: 29, Minerals Production, Vienna 2014
69. Www2.chemie.uni-erlangen.de. (2017). *Vernetztes Studium - Chemie, Chemie for Mediziner: Adsorption*. [online] Available at: http://www2.chemie.uni-erlangen.de/projects/vsc/chemie-mediziner-neu/phasen/adsorption1.html [Accessed 7 Nov. 2016].
70. Xu, P., Zeng, G., Huang, D., Feng, C., Hu, S., Zhao, M., Lai, C., Wei, Z., Huang, C., Xie, G. and Liu, Z. (2012). Use of iron oxide nanomaterials in wastewater treatment: A review. *Science of The Total Environment*, [online] 424. Available at: https://www.ncbi.nlm.nih.gov/pubmed/22391097 [Accessed 8 Oct. 2016].
71. Yazdani, M., Tuutijärvi, T., Bhatnagar, A. and Vahala, R. (2016). Adsorptive removal of arsenic(V) from aqueous phase by feldspars: Kinetics, mechanism, and thermodynamic aspects of adsorption. *Journal of Molecular Liquids*, 214, pp.149-156.